Edinburgh Research Explorer

FLT1 signaling in metastasis-associated macrophages activates an inflammatory signature that promotes breast cancer metastasis

The Journal of Experimental Medicine

FLT1 signaling in metastasis–associated macrophages activates an inflammatory signature that promotes breast cancer metastasis

Bin-Zhi Qian,[1,2] Hui Zhang,[3] Jiufeng Li,[3] Tianfang He,[3] Eun-Jin Yeo,[5,6] Daniel Y.H. Soong,[1] Neil O. Carragher,[2] Alison Munro,[2] Alvin Chang,[4] Anne R. Bresnick,[4] Richard A. Lang,[5,6] and Jeffrey W. Pollard[1,3]

[1]MRC and University of Edinburgh Centre for Reproductive Health, Queen's Medical Research Institute; and [2]Edinburgh Cancer Research UK Centre, MRC Institute of Genetics and Molecular Medicine; University of Edinburgh, Edinburgh EH16 4TJ, Scotland, UK
[3]Department of Developmental and Molecular Biology and [4]Department of Biochemistry, Albert Einstein Cancer Center, Albert Einstein College of Medicine, Bronx, NY 10461
[5]The Visual Systems Group, Abrahamson Pediatric Eye Institute, Divisions of Pediatric Ophthalmology and Developmental Biology, Cincinnati Children's Hospital Medical Center, Cincinnati, OH 45229
[6]Department of Ophthalmology, University of Cincinnati College of Medicine, Cincinnati, OH 45267

Although the link between inflammation and cancer initiation is well established, its role in metastatic diseases, the primary cause of cancer deaths, has been poorly explored. Our previous studies identified a population of metastasis–associated macrophages (MAMs) recruited to the lung that promote tumor cell seeding and growth. Here we show that *FMS–like tyrosine kinase 1* (*Flt1*, also known as VEGFR1) labels a subset of macrophages in human breast cancers that are significantly enriched in metastatic sites. In mouse models of breast cancer pulmonary metastasis, MAMs uniquely express FLT1. Using several genetic models, we show that macrophage FLT1 signaling is critical for metastasis. FLT1 inhibition does not affect MAM recruitment to metastatic lesions but regulates a set of inflammatory response genes, including colony–stimulating factor 1 (CSF1), a central regulator of macrophage biology. Using a gain–of–function approach, we show that CSF1–mediated autocrine signaling in MAMs is downstream of FLT1 and can restore the tumor–promoting activity of FLT1–inhibited MAMs. Thus, CSF1 is epistatic to FLT1, establishing a link between FLT1 and inflammatory responses within breast tumor metastases. Importantly, FLT1 inhibition reduces tumor metastatic efficiency even after initial seeding, suggesting that these pathways represent therapeutic targets in metastatic disease.

CORRESPONDENCE
Jeffrey W. Pollard:
jeff.pollard@ed.ac.uk
OR
Bin-Zhi Qian:
binzhi.qian@ed.ac.uk

Abbreviations used: BMM, bone marrow–derived primary macrophage; IP, immuno-precipitation; IPA, Ingenuity Pathway Analysis; MAM, metastasis–associated macrophage; PlGF, placental growth factor; RFI, relative fluorescence intensity; TAM, tumor-associated macrophage; VEGF, vascular endothelial growth factor.

Breast cancer is the most commonly diagnosed cancer and the second leading cause of cancer death in women. Survival of breast cancer patients has steadily improved because of early screening and adjuvant therapy. Distressingly, however, for women with metastatic disease there has been little change in overall survival over the last 30 yr (Jemal et al., 2010), and it consequently accounts for over 90% deaths from breast cancer (Joyce and Pollard, 2009; Sleeman and Steeg, 2010). This indicates that metastatic breast cancer is largely refractory to current therapeutic strategies. Tumor cell seeding and metastatic growth are the two major rate-limiting steps for distal metastasis (Fidler, 2003). Although mutations in tumor cells account for their acquisition of malignancy, several mechanisms involved in tumor cell extravasation and metastatic seeding are mediated through nontumor-derived microenvironmental factors (Qian et al., 2011; Gil-Bernabé et al., 2012; Labelle and Hynes, 2012; Peinado et al., 2012; Quail and Joyce, 2013).

In the tumor microenvironment, there is compelling evidence that macrophages that infiltrate most cancers promote tumor progression to malignancy and enhance metastasis (Mantovani and Sica, 2010; Qian and Pollard,

Supplemental Material can be found at:
http://jem.rupress.org/content/suppl/2015/08/06/jem.20141555.DC1.html

JEM

2010; Ruffell et al., 2012). At the metastatic site, metastasis-associated macrophages (MAMs) have been shown to stimulate tumor cell extravasation, survival, and subsequent growth in preclinical breast cancer lung metastasis models (Qian et al., 2009, 2011; Chen et al., 2011). Specifically, MAM–derived vascular endothelial growth factor (VEGF) can promote tumor cell extravasation at the metastatic site in part by increased vascular permeability (Qian et al., 2011). As patients usually present with established metastasis, these data argue that targeting the macrophage functions in the metastatic sites could have therapeutic potential (De Palma and Lewis, 2013). However, the mechanisms by which MAMs promote metastatic growth after seeding are still largely unknown.

Detailed immune-phenotyping of cell surface markers indicated that MAMs express a high level of surface FMS-like tyrosine kinase 1 (FLT1) compared with lung-resident macrophages and splenic macrophages (Qian et al., 2009). FLT1 is a family member of VEGF receptor (VEGFR) transmembrane receptor tyrosine kinases that binds to VEGF and placental growth factor (PlGF; Olsson et al., 2006). VEGF plays an important role in tumor progression through its regulation of angiogenesis. However, these effects are largely mediated by VEGFR2 expressed by endothelial cells, and as a consequence of this activity, VEGF and VEGFR2 have been targeted for cancer therapy. In contrast, FLT1 is considered to have minimal signaling activity and largely to be a decoy receptor that titrates VEGF activity (Shibuya, 2006), although in macrophages there is evidence that FLT1 acts as a chemotactic receptor (Murakami et al., 2008; Beck et al., 2010). However, the role of macrophage FLT1 in breast cancer metastasis has not been determined.

In the current study, we show in human breast cancer that FLT1 labels a subset of tumor-associated macrophages (TAMs) and FLT1+ stroma are significantly enriched in breast cancer metastasis samples compared with primary tumors. Combining genetic models of macrophage-specific *Flt1* deficiency and FLT1 inhibitory antibody, we show that FLT1 signaling in MAMs is important for tumor cell survival after metastatic seeding, which suggests that targeting these pathways will have therapeutic efficacy in metastatic disease. Rather than mediating macrophage recruitment, we show a novel activity of FLT1 signaling in regulating a set of inflammatory response genes in the MAMs in vivo. These genes include *colony-stimulating factor 1* (*Csf1*), a major regulator of the mononuclear phagocytic lineage (Chitu and Stanley, 2006) that is up-regulated in breast cancer patients with poor prognosis and metastatic disease (Scholl et al., 1994, 1996; McDermott et al., 2002). Importantly, we show local CSF1 overexpression reverts the inhibitory effect of FLT1 inhibition on tumor cell distal seeding efficiency. Mechanistically, FAK1 acts downstream of FLT1 signaling and regulates CSF1 expression. Thus, our data illustrated a novel mechanism of CSF1-mediated autocrine signaling downstream of FLT1 in macrophages that directly links the inflammatory response with VEGF action and that is critical for the metastasis-promoting function of MAMs.

RESULTS

Host FLT1 signaling is critical for breast cancer metastasis

Flt1tk is a targeted mutation that deletes the tyrosine kinase domain of FLT1 while retaining both the cell surface and secreted form of the receptor. Thus, this mutation ablates FLT1 intracellular signaling capacity but retains its VEGF neutralization capacity, a function that is critical during embryo development (Hiratsuka et al., 1998). To define the role of FLT1 signaling in metastasis, we crossed *Flt1tk* mice with the widely used polyoma middle T (MMTV-PyMT) mouse model for human luminal breast cancers. These mice, whose tumors are caused by the mammary epithelial restricted expression of the PyMT oncogene, recapitulate disease progression in patients with luminal breast cancers and metastasize to lung with high penetrance (Hutchinson and Muller, 2000; Lin et al., 2003). Ablation of FLT1 signaling in the *Flt1tk/tk* homozygous mice does not have a significant effect on PyMT primary tumor burden at 19 wk of age compared with heterozygous littermates (Fig. 1 a). However, metastatic burden (Mets index, defined by percentage of tumor volume in total lung volume using stereological quantification [Qian et al., 2009]) is significantly reduced in the *Flt1tk/tk*-null mutants compared with their heterozygous littermates (Fig. 1, b and c). Both macrophages and endothelial cells express FLT1 in vivo. Previous studies indicated that macrophage–tumor cell paracrine signaling promotes tumor cell migration, which leads to increased tumor cell intravasation and distal metastasis (Condeelis and Pollard, 2006). To test whether FLT1 signaling is involved in promoting tumor cell escape from the primary tumor, we measured the number of circulating tumor cells and found no difference between *FLT1tk/tk* mice and *Flt1tk/+* littermate control (Fig. 1 d). To further test whether macrophage FLT1 signaling is involved in promoting tumor cell migration, we used an in vitro split Boyden chamber assay that measures this effect and did not detect a difference between *Flt1tk/tk* and *Flt1tk/+* littermate control bone marrow–derived primary macrophages (BMMs; Fig. 1 e). Together, these data indicate that FLT1 signaling is critical for spontaneous metastasis but does not affect tumor migration and intravasation in the primary tumor in this model of breast cancer.

Previous studies suggested that FLT1 is a decoy receptor without intrinsic tyrosine kinase activity in endothelial cells attenuating VEGF activity, but it is an active tyrosine kinase receptor in macrophages (Shibuya, 2006). To exclude the involvement of endothelial FLT1 in metastasis, we generated bone marrow mosaic mice using *Flt1tk/tk* mice or *Flt1tk/+* littermates as bone marrow donor in lethally irradiated C57BL/6 mice to restrict the targeted mutation to bone marrow–derived hematopoietic cells (Fig. 1 f). To further confirm our findings, we used another murine breast cancer model in C57BL/6 background, E0771-LG, to perform spontaneous metastasis assay with orthotopic injection, followed by tumor resection when they reach ∼1 cm in diameter 4 wk later in these bone marrow mosaic mice (Fig. 1 f). This hematopoietic-specific genetic loss of function of FLT1 signaling significantly inhibited total pulmonary metastasis burden of E0771-LG
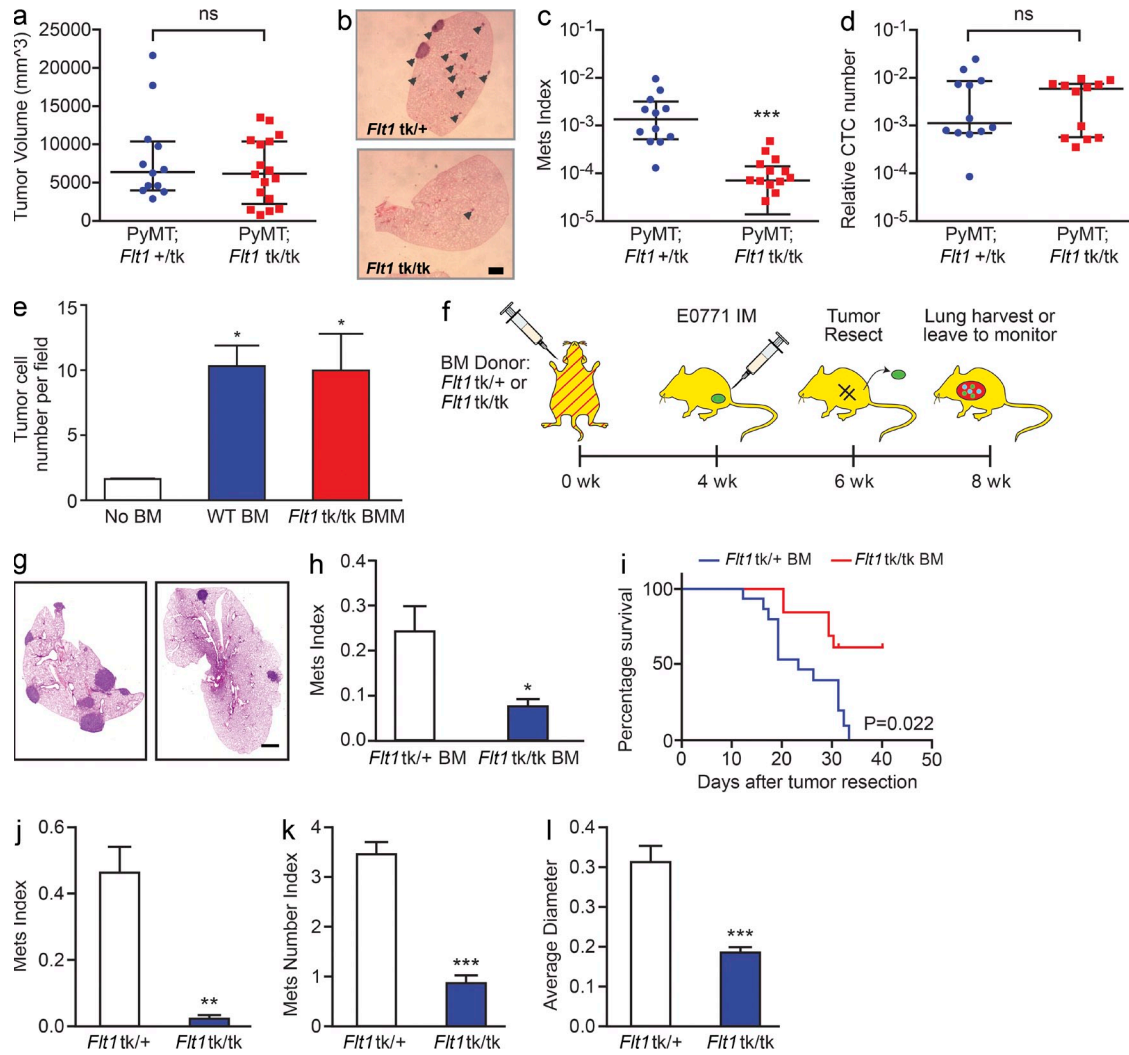
Figure 1.   Stromal FLT1 is important for breast cancer pulmonary metastasis. (a) Total tumor burden of *PyMT;Flt1*$^{tk/+}$ or *PyMT;Flt1*$^{tk/tk}$ mice at 19 wk of age. (b) Representative H&E-stained section of lung metastasis nodules of *PyMT;Flt1*$^{tk/+}$ (top) or *PyMT;Flt1*$^{tk/tk}$ mice (bottom; arrowheads). (c) Stereological quantification of lung metastasis index at 19 wk of age. Mets index is equal to total metastasis volume normalized by total lung volume. Bars show median with interquartile range; $n \geq 12$; ***, $P < 0.001$ by Mann-Whitney test. (d) Quantification of circulating tumor cell number by relative PyMT gene expression in CD45-circulating cells in age-matched littermate mice bearing late stage tumors. Bars represent median $\pm$ interquartile range; $n = 12$; not significant by Mann-Whitney test. (e) BMMs induce Met-1 cell invasion in a modified transwell invasion assay, whereas *Flt1*$^{tk/tk}$ macrophages show no difference compared with WT macrophages. Error bars indicate SEM. $n = 3$ with duplicate; *, $P < 0.05$; not significant between WT and *Flt1*$^{tk/tk}$ BMM by one-way ANOVA with Tukey's multiple comparison. (f) Spontaneous metastasis of E0771 cells in littermate heterozygous or homozygous for *Flt1*^{tk} targeted mutation. (g) Representative automatically stitched scanned images of H&E-stained lung cross section. (b and g) Bars, 1 mm. (h) Stereo-logical quantification of mice harvested at 8 wk. Metastasis quantification was the same as in c. Mean + SEM; $n = 9$; *, $P < 0.05$ by Mann-Whitney test. (i) Survival curve of mice left to monitor. Death is defined as time the mice became moribund; $n \geq 13$; $P = 0.022$ by log-rank test. (j–l) Stereological quan-tification of the distal metastasis efficiency of Met-1 cells in mice heterozygous or homozygous for *Flt1*^{tk} targeted mutation. Mets index (j) was the same as in c; metastasis number index (k) is equal to averaged number of metastasis sites per square millimeter lung area; average diameter (l) is the averaged size of metastasis nodules in millimeters. Bars represent mean $\pm$ SEM. $n \geq 8$; **, $P < 0.01$; ***, $P < 0.001$ by Student's t test.

cells when harvested at 8 wk (Fig. 1, g and h) and significantly prolonged the survival (Fig. 1 i) of these mice compared with their WT controls. These data further confirmed that breast cancer distal metastasis was dependent on host hematopoietic FLT1 signaling.

In spontaneous models, metastasis is the result of distinct metastatic events at the primary tumor and those at the metastatic site. To examine specifically the effect of FLT1 signaling on events at the distal metastatic site (seeding and persistent growth) we performed experimental metastasis (lung colonization) as-says using the PyMT tumor–derived metastatic Met-1 cell line (Borowsky et al., 2005) in *Flt1*$^{tk/tk}$ mice crossed with *Rag2*$^{−/−}$ immune-deficient mice. Deficiency in FLT1 signaling in homozygous *Flt1*$^{tk/tk}$ mice significantly reduced the metastatic
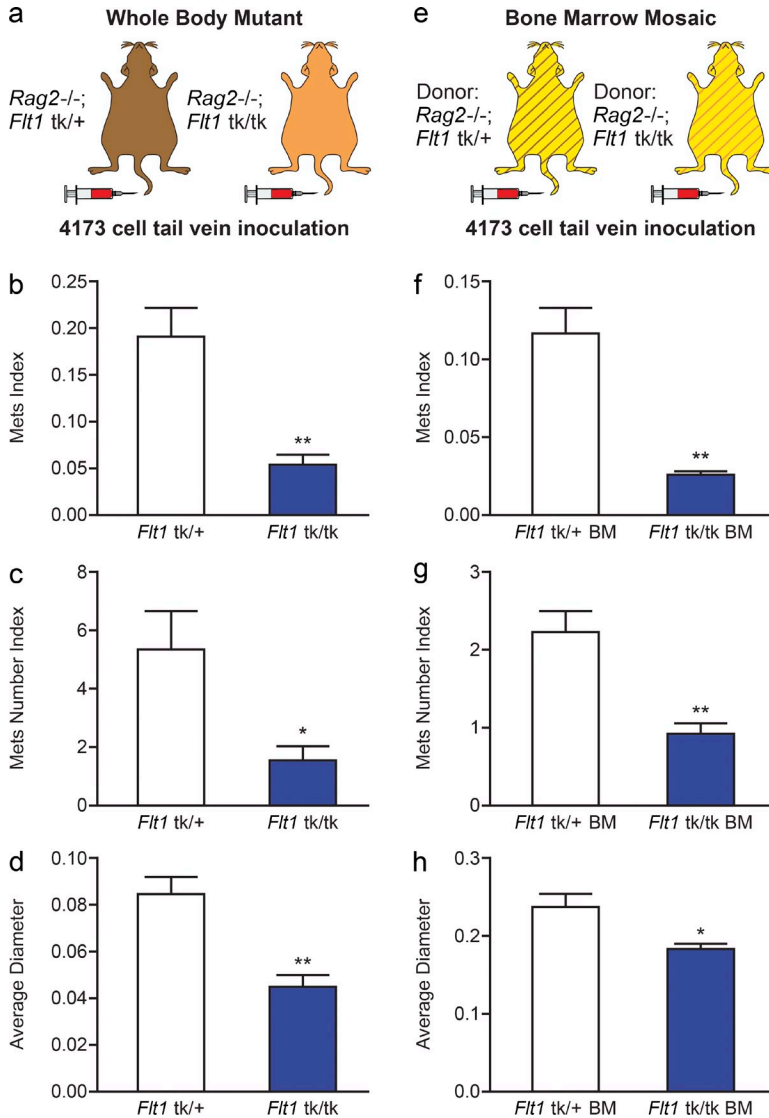
Figure 2. FLT1 tyrosine kinase domain is critical for human breast tumor cell metastasis. (a–d) Experimental metastasis of 4173 cells in $Rag2^{-/-}$ littermate heterozygous or homozygous for $Flt1^{tk}$ targeted mutation with stereological quantification. (e–h) Distal metastasis efficiency of 4173 cells in bone marrow mosaic nude mice with littermate donor of $Rag2^{-/-};Flt1^{tk/+}$ or $Rag2^{-/-};Flt1^{tk/tk}$ mice with stereological quantification. Metastasis quantification was the same as in Fig. 1. Data show mean + SEM. $n \geq 5$; *, $P < 0.05$; **, $P < 0.01$ by Student's t test.

potential of Met-1 cells by ∼90% compared with heterozygous littermates (Fig. 1 j). This is contributed by both the number and size of metastatic nodules that were significantly reduced in the homozygous mutant mice indicated by the metastasis number index and average diameter, respectively (Fig. 1, k and l). Together, our data indicate that FLT1 had a limited role in the primary tumor invasion and intravasation but that both the metastasis rate-limiting steps of seeding and persistent growth at the distal organ of PyMT-induced tumors were dependent on host FLT1 signaling.

Macrophage FLT1 signaling is critical for human breast cancer metastasis

Because the studies in the previous section indicate a role for host FLT1 in metastasis in two independent murine models of breast cancer, we wished to determine whether a similar mechanism is at play with human metastatic breast cancer cells. To this end, we used 4173 cells, the lung trophic derivative of the MDA-MB-231 human breast cancer cell line derived

from a triple-negative patient (Minn et al., 2005; Neve et al., 2006), and tested their dependence for metastasis on host FLT1 tyrosine kinase activity in immune-deficient $Rag2^{-/-}; Flt1^{tk/+}$ and $Rag2^{-/-}; Flt1^{tk/tk}$ mice (Fig. 2 a). The lung metastatic tumor burden of 4173 cells is significantly reduced in $Flt1^{tk/tk}$ mice compared with littermate $Flt1^{tk/+}$ mice (Fig. 2 b). This reduction in metastatic burden was the result of both a reduced number and the size of metastatic nodules (Fig. 2, c and d).

To further exclude the involvement of endothelial FLT1 in human breast cancer metastasis, we used a bone marrow transplant approach to generate mosaic mice using $Rag2^{-/-}; Flt1^{tk/tk}$ mice or $Rag2^{-/-}; Flt1^{tk/+}$ littermates as bone marrow donor in lethally irradiated nude mice (Fig. 2 e). This hematopoietic-specific blockade of FLT1 signaling significantly inhibited the total metastasis burden of 4173 cells compared with control mice (Fig. 2 f). Similar to the data observed with the total body $Flt1^{tk/tk}$ mutants, this inhibition also resulted in reduction in both the number and the size of the metastasis nodules, indicating effects on seeding and persistent growth
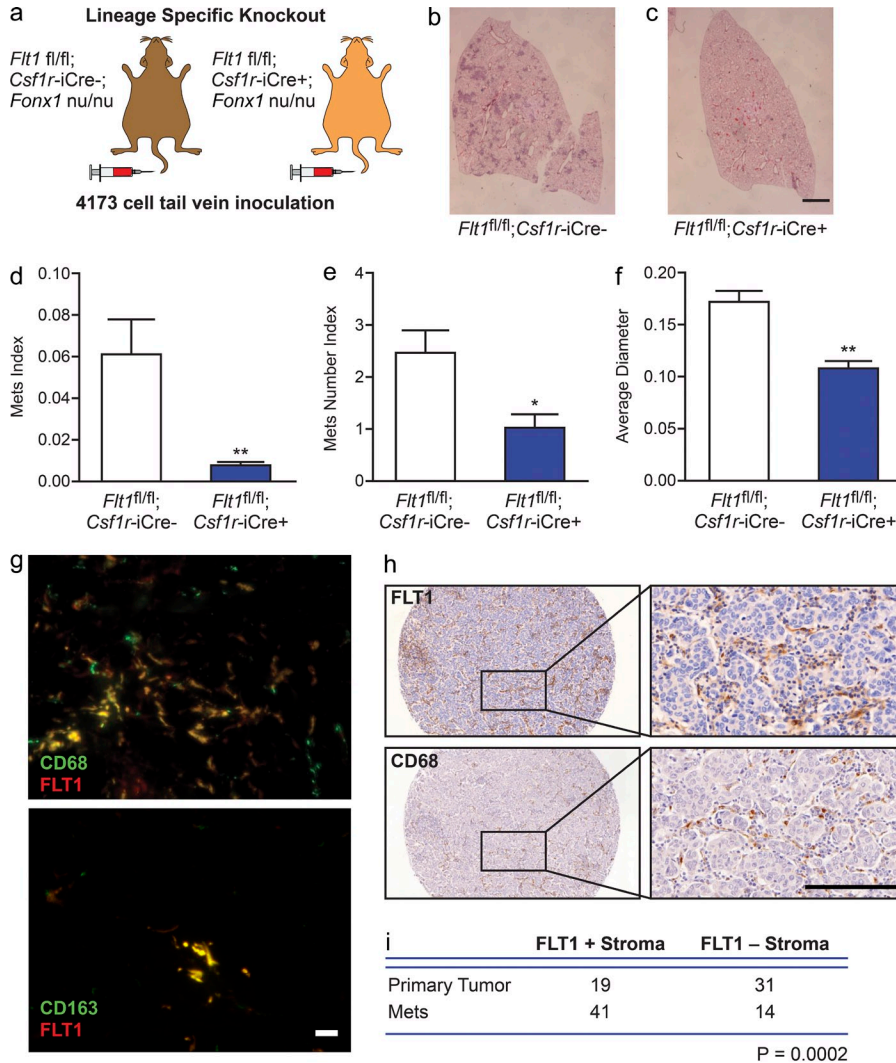
Figure 3. Macrophage–specific FLT1 knockout inhibits human breast tumor cell distal metastasis. (a) Experimental metastasis assay of 4173 cells in nude mice with macrophage-specific *Csf1r-iCre*–induced *Flt1* knockout and *Cre*⁻ littermate controls. (b and c) Representative H&E-stained lung section of lung metastasis in the indicated mice. (d–f) Stereological quantification of the distal metastasis efficiency of 4173 cells in macrophage-specific *Flt1* knockout and littermate control. Metastasis quantification was the same as in Fig. 1. Data show mean + SEM. $n \geq 5$; *, $P < 0.05$; **, $P < 0.01$ by Student's *t* test. (g) Representative micrographs showing colocalization of immunofluor-escently stained FLT1 with macrophage markers using anti-CD68 (top) and CD163 (bottom) antibodies in patient-derived breast tumor samples. (h) Representative FLT1 (top) and CD68 (bottom) immunohisto-chemistry staining–labeled tumor stroma in breast cancer metastasis samples. Bars: (b and c) 1 mm; (g) 20 µm; (h) 100 µm. (i) Number of cases of FLT1-positive (+) and FLT1-negative (-) macrophage-like stroma in primary and metastatic breast cancer samples. P is calculated with Fisher's exact test.

(Fig. 2, g and h). Thus, we can conclude that human meta-static cells are dependent on FLT1 signaling in bone marrow–derived cells for distal seeding and persistent growth.

To confirm the importance of FLT1 signaling in macro-phages in another independent model, we crossed the macrophage-restricted Cre recombinase strain (*Csf1r-iCre*), where the Cre is expressed from the promoter of the *Csf1r* gene (Deng et al., 2010), with *Flt1^flox/flox^* mice to generate macrophage-restricted *Flt1* gene–ablated mice (Stefater et al., 2011). These mice were then bred with nude mice to generate immune-deficient mice that allow metastasis assays of 4173 human breast cancer cells (Fig. 3 a). This Cre-mediated macrophage-specific *Flt1* gene ablation resulted in an ∼90% reduction in the lung metastasis potential of inoculated 4173 cells compared with Cre–negative littermates (Fig. 3, b–d). This inhibition is caused by a reduction in both the number and the size of metastasis nodules (Fig. 3, e and f).

To examine FLT1 expression in macrophages in patient samples of breast cancer, we preformed double immunofluor-escent staining. FLT1 marks the majority (∼80%) of CD68- and

CD163–labeled TAMs by immunofluorescent staining (Fig. 3 g). Using a tissue array that contains 50 cases of primary tumor and 55 metastases, FLT1 was shown to predominantly label macrophage-like stromal cells (CD68⁺) and endothelial cells (Fig. 3 h) and was rarely expressed by tumor cells (3 out of 105 cases). Interestingly, FLT1⁺ macrophages were signifi-cantly enriched in metastases compared with the matched primary tumors, data which suggest these cells may play a role in disease progression (Fig. 3 i). Together, our data indi-cate the FLT1 signaling in MAMs may play an important role for human breast cancer metastasis.

FLT1 inhibition limits persistent growth of established tumor
In light of these results showing an effect of macrophage FLT1 on metastasis growth, we postulated that targeting FLT1 might have therapeutic benefit by inhibiting metastasis. To test this hypothesis, we used a specific monoclonal FLT1–neutralizing antibody (MF1; Wu et al., 2006) to inhibit FLT1 signaling in experimental metastasis assay of Met-1 in syngeneic immune-competent FVB mice in vivo (Fig. 4 a). Consistent with the
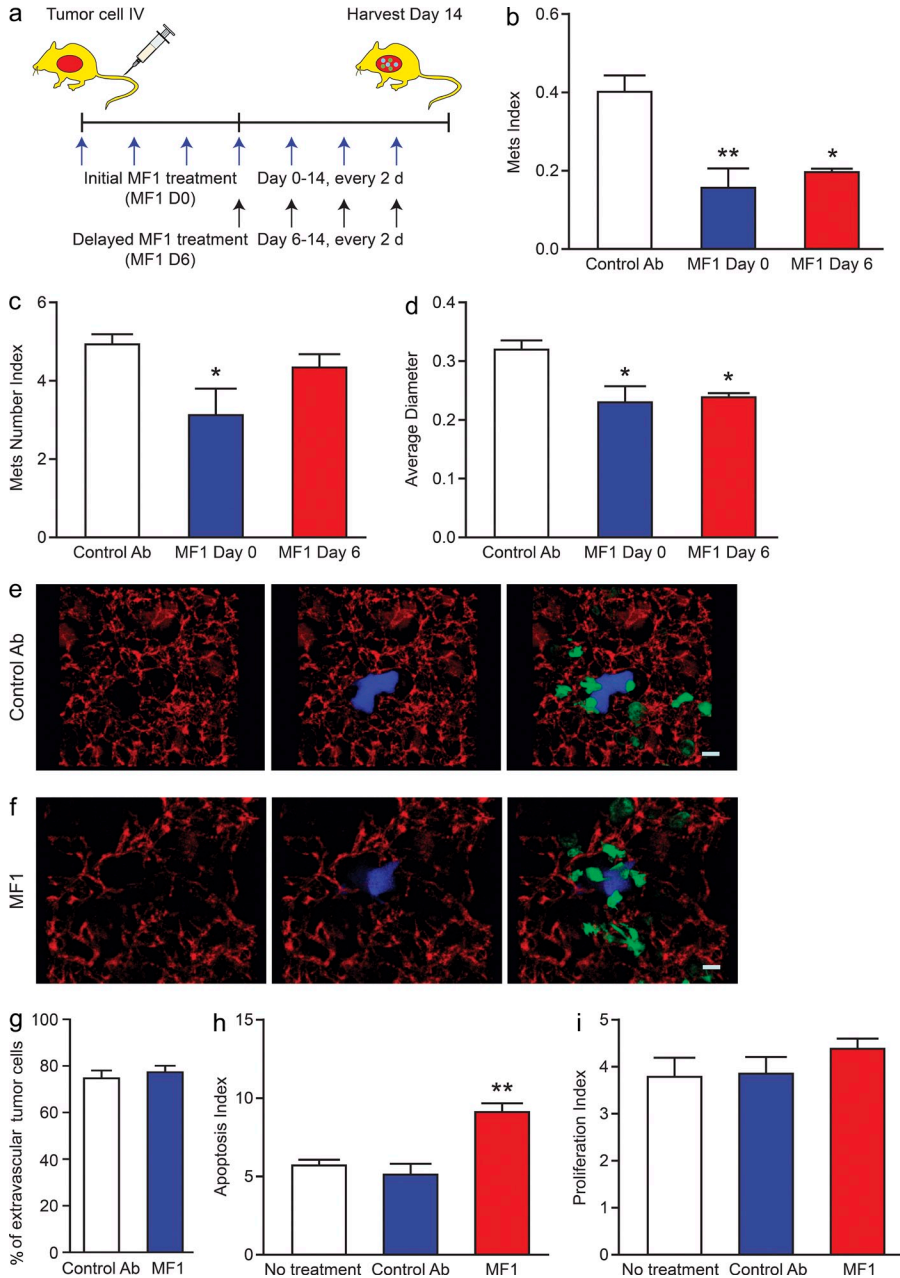
Figure 4. FLT1 inhibition blocks breast cancer metastatic growth. (a) Schematic of experimental metastasis assay of Met-1 cells in syngeneic FVB mice with control antibody and FLT1 inhibitory antibody (MF1) treatment started at the indicated time related to tumor cell inoculation. (b–d) Stereological quantification of the distal metastasis efficiency of Met-1 cells with control and MF1 treatment. Metastasis quantification was the same as in Fig. 1. Mean + SEM. $n \geq 5$; *, $P < 0.05$; **, $P < 0.01$ by ANOVA plus Dunnett's multiple comparison test. (e and f) Representative snapshots of 3D reconstructed confocal images of tumor cell (CFP, shown in blue) and macrophage (GFP, shown in green) 24 h after tumor cell tail vein injection in mice treated with control antibody (e) and MF1 (f). Bars, 200 µm. (g) Quantification of percentage of tumor cells that have extravasated 24 h after tail vein injection. Error bars indicate SEM. $n = 3$; not significant by Student's t test. (h) Apoptosis index, defined by percentage of TUNEL-positive tumor cells, in Met-1 cell lung metastasis with 2-d antibody treatment. Data show mean + SEM. $n \geq 3$; **, $P < 0.01$ by ANOVA plus Dunnett's multiple comparison test. (i) Proliferation index defined by percentage of Ki67-positive cells in total tumor cells. Data are shown as mean + SEM. $n = 4$; not significant by one-way ANOVA.

genetic data descried above, FLT1 inhibition at the time of tumor cell inoculation significantly reduced metastasis efficiency in vivo by targeting both the seeding and persistent growth steps compared with control-treated mice (Fig. 4, b–d, white and blue bars).

The use of FLT1 inhibitory antibody also enabled us to dissect distal metastatic events, i.e., extravasation, seeding, and persistent growth by giving the antibody at different time points according to tumor cell inoculation. In experimental metastasis assays with i.v. inoculated Met-1 cells, the majority of the tumor cells (~75%) have completed extravasation 24 h after inoculation facilitated by direct contact with MAMs derived from CCL2/CCR2 signaling–recruited inflammatory monocytes. Quantification of absolute tumor cell number in lung indicated that the seeding step is estimated to finish at 36 h, defined by the nadir of cell number, and is followed by exponential increase that defines persistent growth (Qian et al., 2009). Using an ex vivo intact lung imaging technique, we found that FLT1 inhibition did not affect tumor cell extravasation and MAM interaction (Fig. 4, e–g). This lack of requirement for extravasation is further confirmed using an in vitro extravasation assay (not depicted) that we established earlier (Qian et al., 2011). These data indicate that FLT1 signaling does not affect tumor cell extravasation during metastatic seeding. In contrast, FLT1 inhibition by MF1 antibody in established Met-1 lung metastasis 6 d after inoculation significantly
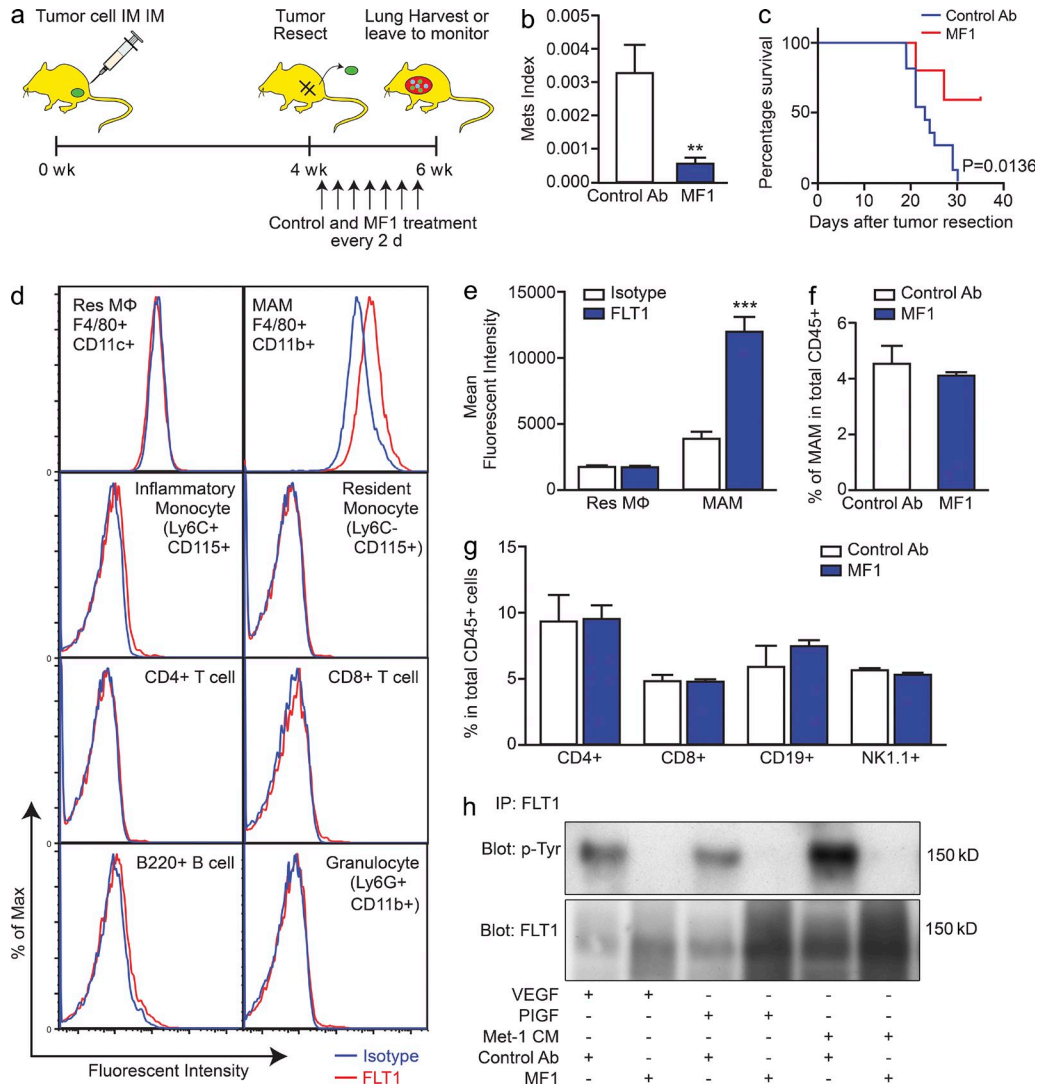
Figure 5. FLT1 inhibition blocks breast cancer metastatic growth. (a) Spontaneous metastasis assay of F246-6 cells with antibody treatment after tumor resection. (b) Stereological quantification of metastasis index (the same as in Fig. 1). Data show mean + SEM. n ≥ 13; **, P < 0.01 by Student's *t* test. (c) Survival curve of mice treated with control or MF1 antibodies. Death is defined when the mice became moribund. n ≥ 10; P = 0.0136 by log-rank test. (d) Representative immunohistograms of the indicated immune cell type showing fluorescent intensity of FLT1 (red) and isotype control (blue) staining. *n* = 3. (e) Mean fluorescent intensity of FLT1 expression in MAMs and lung-resident macrophages. *n* = 3; ***, P < 0.001 using two-way ANOVA followed by Šídák's multiple comparisons test. (f) Percentage of MAMs (F4/80+CD11b+ and Gr1−) in total hematopoietic cells in perfused lung 24 h after Ctrl Ab or MF1 administration. *n* ≥ 3; not significant by Student's *t* test. (g) Percentage of major immune cell populations in total hematopoietic cells in perfused lungs 24 h after Ctrl Ab or MF1 administration. *n* = 3; not significant by Student's *t* test. (e–g) Error bars indicate SEM. (h) Representative Western blot after IP of FLT1 and probing using the p-Tyr antibody in primary macrophages showing phospho-FLT1 (top) and total FLT1 (bottom) treated with the indicated growth factor or tumor cell condition medium. *n* = 3.

inhibited total metastasis burden and average diameter (Fig. 4, b and d, red bars), whereas, as expected, the number of metastatic nodules remained unchanged (Fig. 4 c, red bar). This effect was mainly through an increase in apoptosis of metastatic tumor cells (Fig. 4 h), without an effect on cell proliferation (Fig. 4 i). Treatment of Met-1 cells with MF1 in tissue culture had no effect on their growth, which is in line with their lack of expression of FLT1 (confirmed by both RT-PCR and FACS; not depicted), thereby ruling out direct effects on tumor cells. Together these data indicated that FLT1

signaling in MAMs is critical for the survival of seeded metastatic tumors in our models.

To further test whether inhibition of FLT1 signaling may be effective in treating established metastatic disease, we performed a spontaneous metastasis assay by orthotopic injection of a PyMT-induced mouse mammary tumor cell line, F246-6, in syngeneic FVB mice, followed by tumor resection when they reached ∼1 cm in diameter 4 wk later (Fig. 5 a). FLT1 inhibition after tumor resection significantly inhibited the metastasis burden and prolonged survival (Fig. 5, b and c).

JEM

Together, these data suggest that targeting FLT1 signaling may be effective in treating metastatic breast cancer.

FLT1 modulates inflammatory gene expression in MAMs

To examine cell surface FLT1 expression on bone marrow–derived cells, we used flow cytometric analysis of the major leukocyte populations in immune-competent FVB mice bearing experimentally induced Met-1 cell lung metastasis. MAMs, but not lung-resident macrophages, expressed a significant level of FLT1 (Fig. 5, d and e). Furthermore, Ly6c$^+$ inflammatory monocytes, which are the precursors of MAMs (Qian et al., 2011), do not express FLT1, indicating that this receptor is up-regulated upon differentiation after these precursors have been recruited to the metastatic site (Fig. 5 d). None of the other immune cell types, including Ly6c$^-$ monocytes, granulocytes, nor T or B cells, express FLT1 (Fig. 5 d). Therefore, our data suggest that specific FLT1 signaling in MAMs is critical for metastatic seeding and persistent growth of breast cancer cells in vivo.

FLT1 has been shown to mediate macrophage recruitment; however, FLT1 signaling in macrophages has been poorly explored. Intriguingly, direct measurement by FACS for CD11b$^+$, F4/80$^+$, and Gr1$^-$ MAMs show their recruitment to the lung after Met-1 experimental metastasis was not affected by FLT1 inhibition in vivo (Fig. 5 f). Thus, in the metastatic context, FLT1 does not act as a chemotactic receptor for MAMs, nor does its inhibition affect the recruitment of other major immune cell populations (Fig. 5 g). To determine whether the ligands of this receptor, VEGF and PlGF, activate tyrosine kinase activity in macrophages, we stimulated mouse BMMs that express FLT1 with these ligands and measured tyrosine phosphorylation by anti-FLT1 immunoprecipitation (IP) and Western blotting for phosphor-tyrosine. Both VEGF and PlGF stimulated FLT1 phosphorylation coupled with down-regulation of receptor expression (Fig. 5 h). This is consistent with the behavior of these FMS-like tyrosine kinase receptors that upon ligand binding and activation of the kinase undergo receptor-mediated internalization and destruction (Roth and Stanley, 1992). The efficacy of the MF1 neutralizing antibody was confirmed by the complete inhibition of the kinase activity in its presence in BMMs (Fig. 5 h). We also measured the activity of Met-1–conditioned medium in this IP assay and found that it stimulated FLT1 receptor tyrosine phosphorylation that was also inhibited by MF1. This is consistent with the expression of both VEGF and PlGF by Met-1 cells (not depicted) and suggests that metastatic tumor cells may use these ligands to signal to MAMs in vivo.

These data indicated that FLT1 is not responsible for the recruitment of monocytes or MAMs to the metastatic site and led to the hypothesis that FLT1 modulates the expression of target genes in MAMs to promote metastasis. To identify FLT1-regulated gene expression in MAMs in vivo, we treated mice bearing similar lung metastasis tumor burden of Met-1 cells with control or MF1 antibody. MAMs were FACS sorted based on their distinct cell surface markers and subjected to whole transcriptome microarray analysis (Fig. 6 a). Bioinformatic analysis identified a set of 1,030 unique genes that were differentially regulated by short-term (2 d) FLT1 inhibition, with p-value <0.05 by Student's t test. Among these genes, 688 genes were down-regulated and 342 genes were up-regulated by FLT1 inhibition. Hierarchical clustering with this gene set confirmed the distinct gene expression profile of MAMs with and without FLT1 inhibition (Fig. 6 b). Further bioinformatics analysis with Ingenuity Pathway Analysis (IPA) using information contained in the Ingenuity Knowledge Base identified multiple gene function groups that were significantly enriched in the FLT1-regulated gene set by a right-tailed Fisher's exact test and p-value <0.05 (Fig. 6 c). Interestingly, inflammatory response genes were the most significantly enriched function groups, with all 35 genes in this group differentially regulated by FLT1 inhibition. The majority of these genes encode secreted factors and cell surface molecules, indicating the potential role of FLT1 in regulation of the tumor-promoting function of MAMs by modulating the metastasis microenvironment (Fig. 6 d).

CSF1 acts downstream of FLT1 signaling to promote metastatic growth

Analysis of the IPA data showed that CSF1 has the most interactions with other molecules in the inflammatory response function group (Fig. 6 d). Down-regulation of CSF1 expression by FLT1 inhibition led us to hypothesize that MAMs expressing CSF1 may be required for their function of promoting metastatic growth. To test this hypothesis, we generated bone marrow mosaic mice using lethal irradiation followed by bone marrow transplantation using syngeneic FVB WT donor mice or those homozygous for the *Csf1*-null mutant gene *Csf1^{op}* (Wiktor-Jedrzejczak et al., 1990) and preformed experimental metastasis assay in the mosaic mice using Met-1 cells (Fig. 7 a). In this assay, CSF1 deficiency in bone marrow–derived cells significantly inhibited tumor cell metastatic seeding and persistent growth in vivo (Fig. 7, b–e). This indicates that CSF1 expression by bone marrow–derived cells including macrophages is critical for tumor cell distal metastasis efficiency.

In light of these results, we postulated that if local CSF1 expression by MAMs is critical for tumor cell metastatic efficiency and functions downstream of FLT1 signaling, then a lung-specific induction of CSF1 expression should negate the effect of FLT1 inhibition by the neutralizing antibody, MF1. To test this, a transgenic mouse model allowing lung-specific CSF-1 expression was generated by crossing doxycycline-inducible CSF1 expression mice (*tetO-Csf1*; Van Nguyen and Pollard, 2002) with mice expressing reverse tetracycline-responsive trans-activator (rtTA) under the control of lung-specific *Ccsp* gene promoter (Fig. 7 f; Tichelaar et al., 2000). Experimental metastasis assays were performed in these FVB mice using Met-1 cells treated with MF1 antibody after tumor cell metastatic seeding (4 d after inoculation). Lung-specific CSF1 expression in *Ccsp-rtTA; tetO-Csf1* double transgenic mice induced by treatment with doxycycline significantly restored metastatic growth of Met-1 cells in the presence of
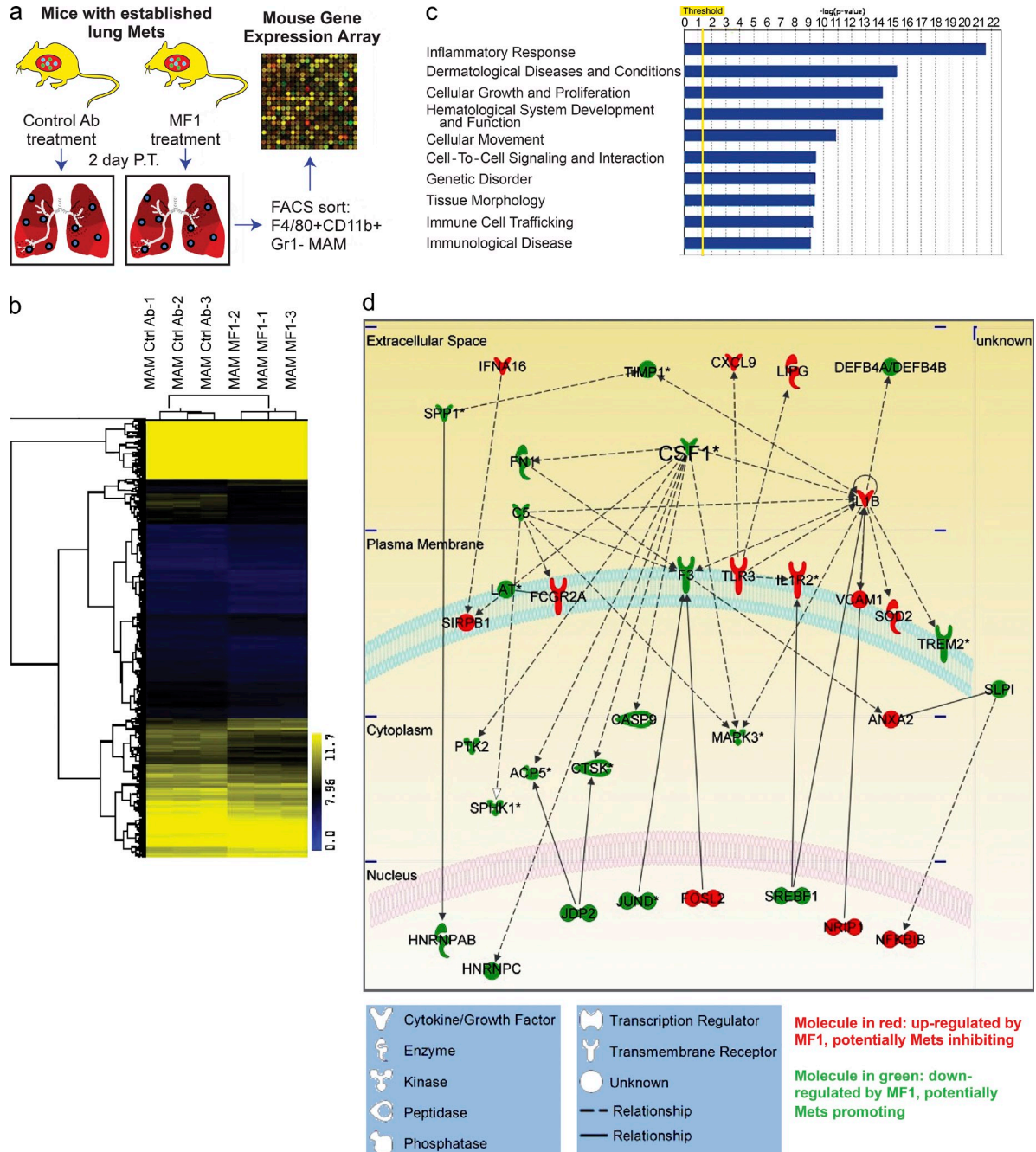
Figure 6.   Transcriptome analysis of FLT1–regulated genes in MAMs. (a) Schematic illustration of microarray transcriptome analysis of FACS-sorted MAMs with control treatment (Ctrl Ab) and FLT1 inhibition (MF1). (b) Hierarchical clustering of FLT1-regulated transcripts distinguishes MAM samples with and without FLT1 inhibition. (c) Top 10 enriched function groups of differentially regulated genes in MAMs with FLT1 inhibition based on IPA. (d) Graphical representation of the molecular relationships of the inflammatory response function group genes enriched in FLT1-regulated transcripts. Molecules are represented as nodes, with the color indicating up (red)- or down-regulation (green) by FLT1 inhibition, and the shape represents the functional class of the gene product as indicated below. The biological relationship between two nodes is represented as a line (solid line: direct interaction, broken line: nondirect interaction). Asterisks indicate CSF1 as one of the gene products that has the most interaction with other gene products in the function group. All interactions are supported by references from the literature in the Ingenuity Knowledge Base.

FLT1 inhibition compared with *tetO-Csf1* single transgenic littermates treated in the same way (Fig. 7, g–i). Because induction of CSF1 expression started after tumor cell seeding, the slight increase of metastasis nodules (although not significant)

may reflect the outgrowth of micrometastasis nodules that were not detectable in the control group (Fig. 7 h). In control mice with no FLT1 inhibition, lung-specific CSF1 overexpression does not change tumor cell metastatic potential
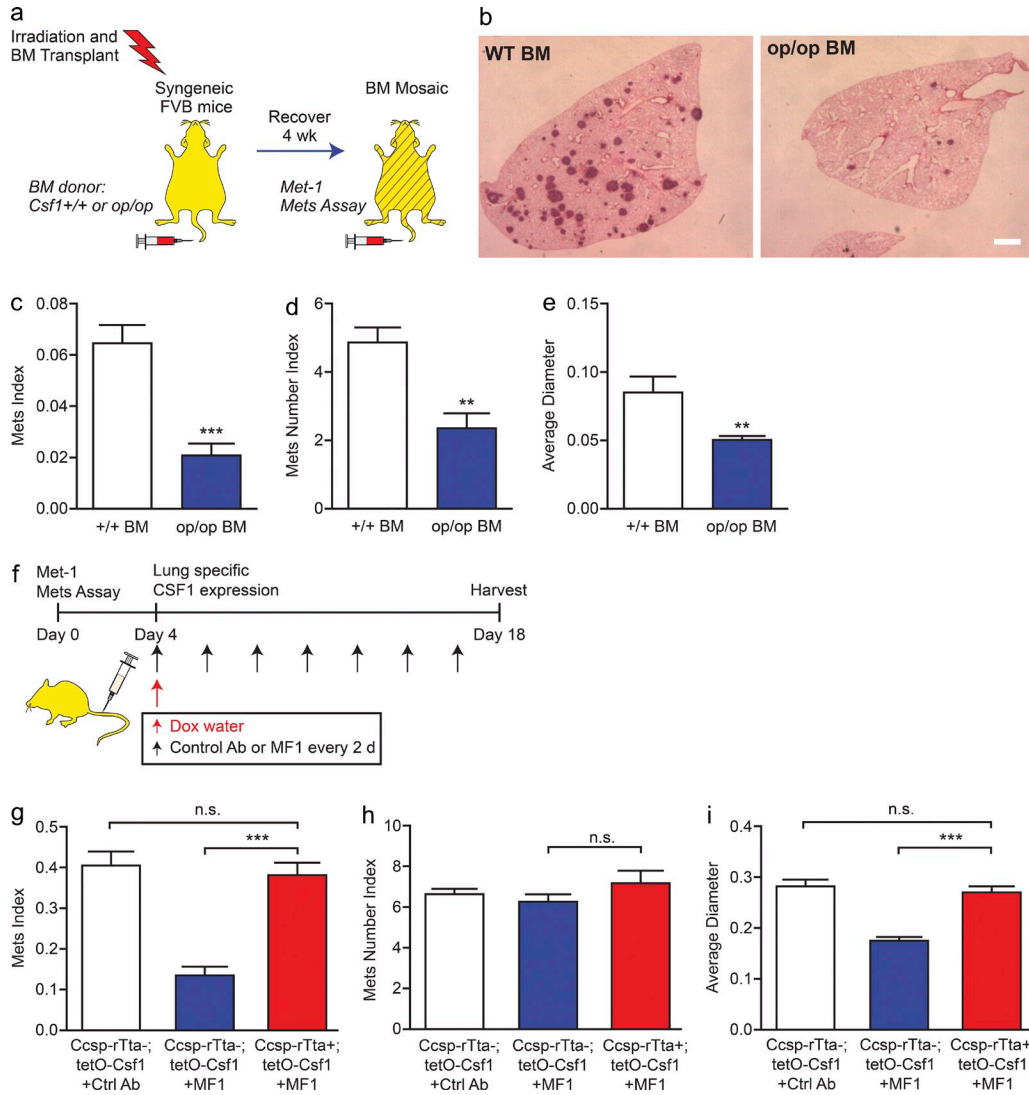
Figure 7. FLT1–regulated CSF1 expression promotes breast tumor cell distal metastasis. (a) Schematic of experimental metastasis assay of Met-1 cells in mosaic mice of bone marrow CSF1-deficient and WT control. (b–e) Representative H&E-stained lung sections (b) and stereological quantification (c–e) of metastatic potential of Met-1 cells in bone marrow mosaic mice as shown in a. *Csf1* WT bone marrow (+/+, white bars) and homozygous null mutant bone marrow (*op/op*, blue bars) are shown. Error bars indicate SEM. $n = 7$; **, $P < 0.01$; ***, $P < 0.001$ by Student's t test. Bar, 1 mm. (f) Schematic of metastasis assay of Met-1 cells with control antibody, FLT1 inhibition (MF1 treatment), and lung-specific doxycycline-inducible CSF1 expression. (g–i) Metastatic potential of Met-1 cells in mice as shown in f. Induced CSF1 expression with MF1 treatment (*Ccsp-rTta +; tetO-Csf1*, red bars) and littermate control (*Ccsp-rTta −; tetO-Csf1*, with control antibody [white bars] or with MF1 [blue bars]). Metastasis quantification was the same as in Fig. 1. Data show mean + SEM. $n \geq 6$; ***, $P < 0.001$ by one-way ANOVA plus Tukey's multiple comparison.

compared with WT mice (not depicted). Together, these data indicated that local CSF1 expression in MAMs acts downstream of FLT1 to promote metastatic growth of breast tumors in vivo.

FLT1 signaling regulates CSF1 expression through FAK1

To further investigate the signaling pathways downstream of FLT1 activation, we used a reverse phase protein array to determine a panel of 45 proteins and phosphor-proteins that covers the major signaling pathways and compared cell lysates of BMMs treated with Met-1 cell–conditioned medium

plus control and MF1 antibodies. FLT1 inhibition most notably modulated the phosphorylation of p38 and FAK1 3 h after treatment (Fig. 8 a, arrows). These results were confirmed by Western blots using anti-p38 and FAK1 antibodies on cell lysates of BMMs from *Flt1*[tk/tk] mice compared with heterozygous littermate control treated with Met-1 cell–conditioned medium (Fig. 8 b). Furthermore, treatment of BMMs with a FAK1-specific inhibitor (FAK inhibitor 14) significantly inhibited tumor cell–conditioned medium–induced CSF1 expression (Fig. 8 c). Together, these data indicate that FAK1 is the potential mechanistic link mediating FLT1 activation to downstream target gene expression.
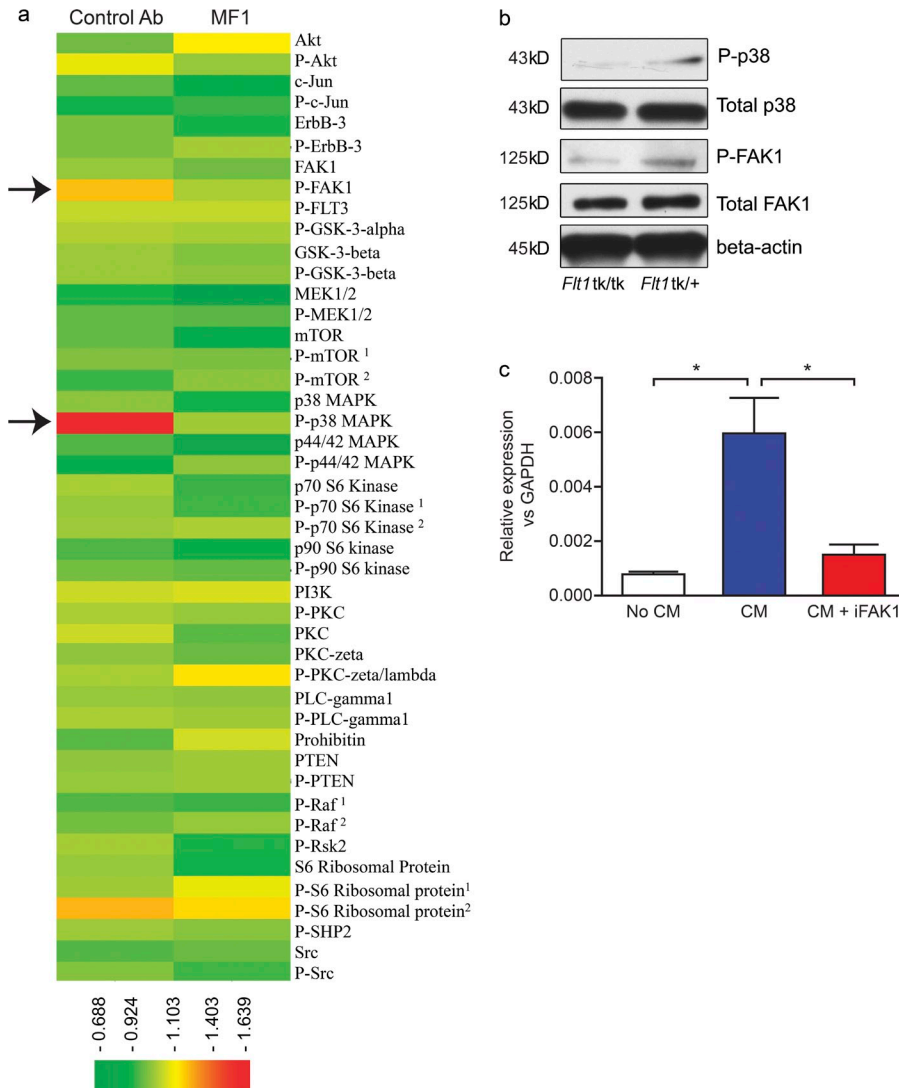
Figure 8. FLT1–regulated CSF1 expression through p–FAK1. (a) Efficacy of FLT1 blockade using MF1 antibody against a panel of 45 proteins and phosphor-proteins on a reverse protein array. Color bar shows relative expression value (global normalization, refer to Table S1 for epitope information). Phosphorylation of p38 and FAK1 show the most notable reduction upon FLT1 blockade using MF1 antibody. $n = 2$. (b) Western blot showing inhibition of phosphor-p38 and phosphor-FAK1 in BMMs from littermate mice heterozygous or homozygous for $Flt1^{tk}$. Representative blot from two independent experiments. (c) FAK1 inhibitor blocks tumor cell–conditioned medium (CM)–induced mRNA $Csf1$ expression in BMMs. Data show mean + SEM. $n = 3$; *, $P < 0.05$ by ANOVA plus Dunnett's multiple comparison test.

DISCUSSION

Compelling recent evidence indicated that TAMs are critical for metastatic progression in tumors (Mantovani and Sica, 2010; Qian and Pollard, 2010). Studies, particularly in but not limited to, breast cancer (Lin et al., 2001; Coussens and Pollard, 2011) show these macrophages actions are at all stages in the metastatic cascade, including promotion of tumor cell migration and escape into the circulation (Wyckoff et al., 2007) and their subsequent extravasation, survival, and persistent growth at target organs (Qian et al., 2011). Our studies showed that macrophages associated with distal metastasis were derived from a subset of circulating CCR2-expressing Ly6c^{+} monocytes upon CCL2 chemokine signaling and enhance tumor cell extravasation (Qian et al., 2011). Blockade of CCL2 signaling inhibited MAM recruitment to metastatic sites, reduced metastasis, and prolonged survival of mice (Qian et al., 2011). These MAMs also promote tumor cell survival through direct contact mediated by VCAM1 (Chen et al., 2011), and their retention in metastasis is mediated by a CCL3 autocrine

signaling downstream of CCL2 (Kitamura et al., 2015). In the current study, we illustrated a new mechanism of metastasis-promoting function of MAMs mediated by FLT1 receptor tyrosine kinase signaling, which may offer a new therapy target in treating metastatic disease of breast cancer.

Immunoprofiling of cell surface markers indicated that MAMs express high levels of FLT1. During angiogenesis, FLT1 generally acts in a kinase–independent manner as a decoy receptor titrating the proangiogenic factor VEGF with a 10-fold higher affinity compared with VEGFR2 (Shibuya, 2006). In this role, FLT1 can be expressed by both endothelial cells (Hiratsuka et al., 1998) and macrophages (Stefater et al., 2011). There is also evidence that its tyrosine kinase signaling activity can recruit myeloid cells in developmental and tumor graft settings (Murakami et al., 2008). In this study, using a genetically modified mouse model, we showed that FLT1 signaling is critical for spontaneous lung metastasis in immune-competent mice. Furthermore, we demonstrated that macrophage FLT1 is essential for tumor cell seeding and persistent

growth during distal metastasis. These experiments included two independent models of lineage FLT1 ablation (*Flt1^flox/flox*; *Csf1r-iCre*) and FLT1 kinase domain knockout (*Flt1^tk*) in combination with bone marrow transplantation to confirm the requirement for FLT1 signaling for these protumoral functions through its tyrosine kinase domain in macrophages. Our previous study (Qian et al., 2011) established an essential role for monocyte-derived VEGF through its ability to enhance vascular permeability. This VEGF production by monocytes and the expression of FLT1 on MAMs suggest, in addition to its effects on endothelial cells, an autocrine role that together with tumor cell–expressed VEGF may synergize in the metastatic site to cause differentiation of the incoming monocytes to metastasis-promoting MAMs and their subsequent ability to promote metastatic growth.

Our data show that *Flt1^tk/tk* mutation does not affect primary tumor growth in the PyMT model of breast cancer. However, inhibition of the FLT1 ligand PlGF has been reported to inhibit tumor growth in the transplanted B6 melanoma and Panc02 models (Fischer et al., 2007). In contrast to this data, other studies using several different anti–PlGF antibodies or the *Flt1^tk/tk* mutant failed to show inhibition of tumor growth in the same or in other transplantation models (Bais et al., 2010) or in GEM models of pancreatic cancer (Casanovas et al., 2005). These data suggest that the originally published observations with a single antibody might be the result off-target effects (Bais et al., 2010).

However, FLT1-expressing myeloid cells have been shown to play a role in metastasis. These FLT1-positive myeloid cells educated by the primary tumor have been shown to precondition sites, known as premetastatic niches, distant to the tumor that enhance metastatic seeding in experimental metastasis models (Hiratsuka et al., 2002; Kaplan et al., 2005). These cells promote metastasis through MMP9 expression as well as enhancing fibronectin deposition that have the combined effect of promoting tumor cell adhesion and therefore metastatic seeding (Hiratsuka et al., 2002; Kaplan et al., 2005; Dawson et al., 2009a). Inhibition of FLT1 with MF1 antibody or in the *Flt1^tk/tk* genetic background inhibited these actions and blocked metastasis (Kaplan et al., 2005). Furthermore, inhibition of clotting inhibited recruitment of the CD11b⁺ and F4/80⁺ cells and ablated the metastatic niche. Nevertheless, even in the presence of clotting, CD11b⁺ macrophage ablation inhibited metastasis, indicating the central importance of the myeloid cell recruitment to metastatic enhancement (Gil-Bernabé et al., 2012). In direct contrast to these studies in a tumor resection model, Dawson et al. (2009b) were unable to inhibit metastasis in the LLC or B16 melanoma model with either MF1 antibody or in the *Flt1^tk/tk* mutant mice. However, these studies relied on tumor resection by hind-limb amputation that might have perturbed the systemic environment or showed the continuing need for a primary tumor to maintain the effect. However, in experimental pulmonary metastasis assays using B16F10 cells that by definition lack an initiating tumor, a reduction of metastasis was observed by inhibition of FLT1 using either anti–PlGF antibodies or *Flt1^tk/tk*

mice (Bais et al., 2010). These data are consistent with those presented here for breast cancer models where we show in both spontaneous PyMT model and three different mouse and human experimental syngeneic or transplanted models that inhibition of FLT1 signaling either genetically or by antibody inhibition markedly reduced pulmonary metastasis. Furthermore, in two independent syngenic models where we resected the primary tumor in the *Flt1^tk/tk* bone marrow chimeric background or followed by MF1 treatment, we also observed inhibition of spontaneous metastasis. Importantly, our data in these models showed improved survival of the mice after FLT1 inhibition. Furthermore, we identified expression of FLT1 in macrophages in human breast cancer metastasis that was significantly enriched at these sites compared with the primary tumor.

Interestingly, in our models of breast cancer metastasis, FLT1 is specifically expressed by MAMs but not by monocytic precursors or lung-resident macrophages, and FLT1 inhibition did not affect their recruitment. This is different from previous studies showing that FLT1 signaling mediated macrophage recruitment in response to pathogens and to gliomas in a xenograft model (Murdoch et al., 2004; Murakami et al., 2008). In addition, CD45⁺c-Kit⁺ or Sca-1⁺ hematopoietic progenitor cells were reported in models of melanoma and lung carcinoma (Lyden et al., 2001) but were very rare (<0.05% of total CD45⁺ cells) in metastasis-bearing lungs in the current study and did not change with FLT1 inhibition (unpublished data). Instead, in parallel to the inhibition of tumor cell metastatic potential by FLT1 inhibitory antibody (MF1), FLT1 phosphorylation induced in macrophages by its ligands and by tumor cell–conditioned medium was significantly blocked. This indicated that FLT1 inhibition by MF1 may alter the metastasis-promoting function of MAMs by deregulating downstream target genes. Indeed, using transcriptome analysis, we identified an FLT1-regulated gene expression signature dominated by inflammatory response genes in MAMs in vivo.

A set of inflammatory response–related genes are the most significantly enriched gene function group in FLT1-regulated genes. Among which, CSF1 is significantly down-regulated by FLT1 inhibition, suggesting a role for macrophage-synthesized CSF1 in metastasis promotion. CSF1 is a key cytokine for macrophage function in vivo being required for macrophage survival, proliferation, and differentiation, as well as being chemotactic to these cells (Chitu and Stanley, 2006). Our data showed that CSF1 expression in response to FLT1 signaling is critical for breast tumor metastatic seeding and growth. Because CSF1 receptor is restricted to monocytes/macrophages in adult mice (Byrne et al., 1981), these data indicate a novel CSF1-mediated autocrine signaling in MAMs downstream of FLT1. Importantly, using a lung-specific gain-of-function tetracycline-regulated system, we showed that lung-restricted CSF1 expression reverts the inhibitory effect of FLT1 inhibition by MF1 on metastatic growth. This provides genetic evidence for CSF1 being epistatic to FLT1 in MAMs. CSF1 in turn has been shown to stimulate VEGF production in macrophages (Curry et al., 2008), suggesting a positive feedback

loop. These findings provide a mechanistic basis for the clinical observations that CSF1 expression is associated with poor prognosis and metastatic disease in breast cancer patients (Scholl et al., 1994, 1996; McDermott et al., 2002). Similar correlations were found for endometrial, ovarian, and prostatic cancers, suggesting that similar FLT1-mediated mechanisms may be at play in the metastasis of these cancers (Smith et al., 1995; Toy et al., 2001; Richardsen et al., 2008).

There is now substantial evidence that inflammation plays a critical role in promoting tumorigenesis and in the subsequent progression of tumors to malignancy (Mantovani et al., 2008; Grivennikov et al., 2010; Coussens et al., 2013). In fact, every solid cancer appears to invoke an inflammatory response, and in contrast to original concepts, this reaction is largely tumor promoting. However, little is known about the mechanisms by which inflammatory responses influence metastasis. In this study, FLT1 blockade inhibits spontaneous metastasis after primary tumor removal and metastatic seeding and prolonged survival. Importantly, we define a novel coupling of FLT1 signaling in macrophages to the regulation of an inflammatory response at the site of metastatic seeding and growth. This response includes the important macrophage survival and differentiation factor CSF1 that, through an autocrine action in macrophages, promotes metastasis. These data provided a strong rationale for jointly targeting VEGF and CSF1R in patients to break this positively reinforcing autocrine loop and curb metastatic disease.

MATERIALS AND METHODS

Animals studies. All procedures involving mice were conducted in accordance with National Institutes of Health regulations concerning the use and care of experimental animals. The study of mice was approved by the Albert Einstein College of Medicine Animal Use Committee. Transgenic mice expressing the PyMT oncogene under the control of MMTV LTR were provided by W.J. Muller (McMaster University, Hamilton, Ontario, Canada) and bred in house in FVB background. C57BL/6 *Flt1*$^{tk/tk}$ (Hiratsuka et al., 1998), C57BL/6 *Flt1*$^{flox/flox}$ (Ambati et al., 2006), and FVB *Ccsp-rTta* (Tichelaar et al., 2000) mice were provided M. Shibuya (University of Tokyo, Tokyo, Japan), N. Ferrara (Genentech, South San Francisco, CA), and J. Wittset (University of Cincinnati, Cincinnati, OH), respectively. MMTV-PyMT; *Flt1*^{tk} were generated in house by crossing two strains and maintained by intercross. *Flt1*^{tk} were also crossed with Rag2$^{-/-}$ (obtained from Charles River) to generate mice in immune-deficient background for metastasis assay using human breast cancer cells, 4173, or cells in FVB background, Met-1. The FVB *Ccsp-rTta* were crossed with *tetO-Csf1* mice generated by our group previously (Lin et al., 2001). For generation of bone marrow mosaic mice, recipient mice at 3 wk of age were irradiated with gamma irradiation at 8 Gy to deplete endogenous hematopoietic cells and rested for 5 h before i.v. injection of total bone marrow cells from donor mice for reconstitution. These mice were then recovered for 4 wk before metastasis assays (see Experimental and spontaneous metastasis assay). FLT1-neutralizing antibody (MF1) was provided by ImClone Systems, a wholly owned subsidiary of Eli Lilly & Co. Antibodies were given at 40 mg/kg body weight via i.p. injection every 2 d at days indicated in Fig. 4 a according to tumor cell inoculation. Control rat IgG (EMD Millipore) was administered at the same schedule. All in vivo experiments were at least two independent experiments with three to five mice for each group.

Human tissue array and immunohistochemistry. Tissue array of breast carcinoma and matched lymph node metastasis were obtained from US Biomax, Inc. Antibodies used were anti–human FLT1 (Novus Biologicals),

anti–human CD68 (Dako), and anti–human CD163 (AbD Serotec). Immunohistochemistry/immunofluorescence were performed using protocols recommended by the antibody providers. FLT1 staining was scored manually in a blinded fashion by an independent investigator, and no staining was scored as negative.

Cell culture and Western blot. E0771, mouse mammary adenocarcinoma, cells were provided by E. Mihich (Roswell Park Cancer Institute, Buffalo, NY). Highly metastatic populations, E0771-LG, were obtained by in vivo selection of lung metastatic cells after i.v. injection in syngeneic C57BL/6 mice (Kitamura et al., 2015). F246-6 cells were derived from a late-stage mouse mammary tumor from MMTV-PyMT mice in syngeneic FVB background and showed high metastatic potential after orthotopic implantation. All cells were cultured in DMEM supplemented with 10% FBS. Proliferation assays were performed in the presence of 30 µg/ml MF1 and control antibody, and cell numbers were counted using Guava (EMD Millipore) at the indicated time point. BMMs were differentiated from bone marrow progenitor cells in the presence of 100 ng/ml CSF-1 for 7 d before being treated with FLT1 ligand or tumor cell condition medium (1:4 diluted in fresh medium) for 30 min. FLT1 was immunoprecipitated from total cell lysate using an anti-FLT1 antibody (Santa Cruz Biotechnology, Inc.), and tyrosine phosphorylation was detected using phospho-tyrosine antibody (Cell Signaling Technology). FAK1 and p38 antibodies for Western blotting were the same as those used in the protein array (Table S1). BMMs were treated with Met-1 cell–conditioned medium and FAK inhibitor 14 (10 µM final concentration; Sigma-Aldrich) before RNA was harvested for real-time PCR analysis to determine mRNA *Csf1* expression. Primers used were the following: *Csf1*, 5′-CTCATCTGGGATCCTCTCCA-3′, 5′-TGTCAA-AAGGTGGCATTTCA-3′; and *Gapdh*, 5′-CCATCACCATCTTCCAG-GAG-3′, 5′-TCTCCATGGTGGTGAAGACA-3′.

Modified transwell invasion assay. 10^5 BMMs were plated in 24-well plates in complete M3 medium and incubated overnight. The BMMs were rinsed twice with PBS, and the medium was then changed to serum-free M3 medium (containing 120 ng/ml CSF-1); control wells contained the same medium without macrophages. Transwell chambers coated with growth factor–reduced (GFR) Matrigel (8-µm pore; #354483; BD) were rehydrated for 2 h at 37°C. 3 × 10^4 tumor cells, which had been serum starved for 5 h, were plated in the upper chamber of the transwell. Tumor cells were allowed to invade for 24 h at 37°C. The transwell inserts were fixed with 4% paraformaldehyde for 15 min, and the cells on the upper surface were removed with a cotton swab. The inserts were stained with Hoechst and rinsed five times with PBS, and the membranes were mounted on glass coverslips using Mowiol. 10 random fields at 10× magnification per membrane were imaged, and the cells were counted using ImageJ (National Institutes of Health). Three independent experiments with duplicate transwells were performed.

Transendothelial cell migration assay. Transendothelial migration assay was performed as described previously (Qian et al., 2011). In brief, 10^4 endothelium cells, 3B-11 (ATCC), were plated into the upper chamber of a GFR Matrigel invasion chamber (BD) in DMEM with 10% FBS. A monolayer was formed in 2 d and verified by microscopy. 10^4 BMMs or FACS-sorted monocytes were loaded to the basolateral side of the insert and put into the plate well with DMEM with 10% FBS and 10^4 U/ml CSF-1 to allow attachment. 2 × 10^4 CellTracker CMRA (Invitrogen)–stained Met-1 cells were loaded into the insert with DMEM in 0.5% FBS and 100 ng/ml CSF-1. FLT1 neutralizing antibody and control antibody were used at a concentration of 10 µg/ml to both sides of the insert. Plates were incubated under normal tissue culture conditions for 48 h before being fixed with 1% (wt/vol) paraformaldehyde. Quantification of transmigrated tumor cells was the same as described in the invasion assay in the previous section.

Experimental and spontaneous metastasis assay. 8-wk-old FVB females or 6-wk-old female nude mice were used for all experimental metastasis assays with 5 × 10^5 PyMT-induced tumor cells, Met-1, and 10^6 MDA231-derived

JEM

human tumor cells, respectively. If not specified, all animals were sacrificed 2 wk after i.v. injection of PyMT cells or 4 wk for human tumor cells for optimal metastatic burden. 10^6 E0771-LG or F246-6 cells were injected into the fat pad of fourth mammary gland of C57BL/6 or FVB mice, respectively, at 7–8 wk of age to establish primary tumor. These tumors were then surgically removed when reaching 1 cm in diameter in ∼4 wk. Metastasis was allowed to develop for another 2 wk before harvesting lungs. For paraffin sections, before removal, lungs were injected with 1.2 ml of 10% (vol/vol) neutral buffered formalin by tracheal cannulation to fix the inner airspaces and inflate the lung lobes. Lungs were excised and fixed in formalin overnight. A precise stereological method (Nielsen et al., 2001) with slight modification was used for lung metastasis quantification. In brief, paraffin-embedded lungs were systematically sectioned through the entire lung with one 5-µm section taken in every 0.5-mm lung thickness. All the sections were stained with hematoxylin and eosin (H&E), and images were taken using an AxioScan.Z1 slide scanner (Carl Zeiss) and analyzed using Tissue Studio (Definiens; Figs. 2 and 5 h) or SV11 microscope (Carl Zeiss) with a Retiga 1300 digital camera (QImaging) and analyzed using ImageJ software (all other figures). As described earlier (Qian et al., 2009), three parameters (Mets index, Mets number index, and average diameter) were calculated to estimate total metastasis burden, seeding efficiency, and metastatic growth, respectively. Mets index is defined by the percentage of metastatic tumor volume in total lung volume. Mets number index is defined by number of tumor nodules per square millimeter of lung area, and average diameter of all tumor nodules is the average diameter in millimeters. Please note that the difference in volume is proportional to the cube of the difference in diameter.

FACS analysis. For FACS analysis, lungs were perfused briefly with cold PBS before harvest, minced on ice, and then digested with an enzyme mix of Liberase and Dispase (Invitrogen). Cells were blocked using anti–mouse CD16/CD32 antibody (eBioscience) for mouse cells or 10% goat serum for human cells before antibody staining. Antibodies used are the following: anti–mouse CD45 (30-F11), CD11b (M1/70), Gr1 (RB6-8C5), FLT1 (141522; R&D Systems); CD4 (GK1.5), CD8a (53-6.7), CD19 (1D3), CD115 (AFS98) Nk1.1 (PK136; eBioscience); and F4/80 (Cl:A3-1; AbD Serotec). FACS analysis was performed on an LSRII cytometer (BD), and data were analyzed using FlowJo software (Tree Star). Single cell gating using FSC/W and SSC/W and dead cell exclusion with DAPI staining were performed routinely during analysis.

FACS sorting of specific macrophage populations and gene expression array analysis. Fluorescently labeled antibodies and tissue preparation were the same as described for the FACS analysis in the previous section. Metastasis-recruited macrophages (F4/80^{+}CD11b^{+}Gr1^{−}) were sorted from lungs bearing experimental metastasis of Met-1 cells using a MoFlo (Dako). In each sample, purity was >98% by post-sort analysis. Total RNA was extracted from these sorted macrophages (RNeasy Mini kit; QIAGEN), and its quality was determined using Pico Chip with a 2100 Bioanalyzer (Agilent Technologies). High-quality RNA was amplified one round using a MessageAmp II aRNA kit (Ambion) and reverse-transcribed into double-strand cDNA. Samples where then submitted to NimbleGen for labeling and hybridization on their mouse gene expression array (MM8). Two-tailed Student's t test was used to analyze the gene expression values with TM4 MeV microarray software suite (Saeed et al., 2003). Genes had 1.5-fold change and P < 0.05 in mean expression values in MAMs compared with FLT1 inhibition and control treated. Original data were deposited at Gene Expression Omnibus (accession no. GSE68843).

Bioinformatics. The Database for Annotation, Visualization and Integrated Discovery (DAVID), the NCBI Entrez Gene and Gene Reference into Function, the Mouse Genome Informatics, and extensive literature review were used for annotating regulated transcripts with precise gene ontology designation. Function gene group analyses were performed with IPA software (Ingenuity Systems).

Reverse phase protein microarray. Quantification of the abundance of total protein and phosphorylated protein epitopes were calculated using the Zeptosens reverse phase protein microarray platform. After incubation of BMM cultures with Met-1–conditioned media with control antibody or MF1 incubation, cells were rinsed twice in ice-cold PBS and lysed in the CLB1 lysis buffer (Bayer Technology Services) at room temperature for 30 min. Lysates were collected and centrifuged in microcentrifuge at 14,000 rpm for 5 min. Supernatants were collected and subjected to total protein determination, and lysates were normalized to 1 mg/ml concentration.

Before spotting cell lysates onto ZeptoMARK hydrophobic chips (Zeptosens), samples were diluted fivefold with CSBL1 spotting buffer (Zeptosens) to generate the primary spotting solution and then further diluted with 90% CSBL1/10% CLB1 to obtain four different protein concentrations corresponding to 100, 75, 50, and 25% of the primary spotting solution. For each of these four dilutions, individual spots were arrayed onto ZeptoMARK hydrophobic chips as single sample droplets of ∼400 pl, using a noncontact spotter equipped with piezo-electric microdispensers (Nano-Plotter NP2.1; GeSiM). After spotting, the chips were dried for 1 h at 37°C, blocked in an ultrasonic nebulizer (ZeptoFOG; Zeptosens) with CeLyA Blocking Buffer (BB1; Bayer Technology Services). Blocked chips were rinsed extensively with water (Milli-Q quality) and dried by centrifugation at 200 g for 5 min.

Using the built-in microflow ZeptoCARRIER system (Zeptosens, Bayer Technology Services), the arrays were incubated with a panel of 45 primary antibodies (Table S1) overnight at room temperature. After rinsing the system with assay buffer, the secondary detection antibodies (anti–rabbit and isotype-specific anti–mouse Alexa Fluor 647) were applied to appropriate subarrays for 2.5 h at room temperature in the dark. The excess secondary antibody was removed by washing with assay buffer, and fluorescence readout of the arrays was performed on the ZeptoREADER (Zeptosens) at an extinction wavelength of 635 nm and an emission wavelength of 670 nm. The fluorescence signal was integrated over a period of 1–10 s, depending on the signal intensity. Array images were stored as 16-bit TIFF files and analyzed with the Zepto-VIEW Pro software package (version 3.1; Zeptosens, Bayer Technology Services). Each sample 4-point concentration series is spotted onto the microarray chip between Alexa Fluor–conjugated BSA standards. Fluorescence intensity signals of each sample are calculated by optimized image analysis algorithms and normalized to intensity values of BSA standards through a local 2D quadratic function. A single relative fluorescence intensity (RFI) value was obtained by a weighted linear fit through sample dilutions representing the relative protein abundance across the sample series.

A panel of 45 protein analysts (see Table S1) were normalized by the following global normalization procedure using the entire antibody panel. (a) Determine median for each antibody across the sample set. (b) Divide each raw linear value by the median within each antibody to obtain the median-centered ratio. (c) Calculate the median from median-centered ratio for each sample across the entire panel of antibodies. This median functions as a correction factor (COMPARE1) for protein loading adjustment. (d) Divide raw RFI data by the correction factor to obtain the normalized values. Global normalized data were used to generate a heat map. In addition, RFI ratios of phosphorylated p38 MAPK and phosphorylated FAK modifications to total protein were calculated by the ZeptoVIEW 3.1 software (Zeptosens) and plotted as bar graphs.

Statistical analysis. Unless specified otherwise, statistical analysis methods used were standard two-tailed Student's t test for two datasets and ANOVA followed by multiple comparison tests for multiple datasets using Prism (GraphPad Software); p-values <0.05 (*), <0.01 (**), and <0.001 (***) were deemed as significant.

Online supplemental material. Table S1, included in a separate PDF file, lists antibodies used in the reverse phase protein array. Online supplemental material is available at http://www.jem.org/cgi/content/full/jem .20141555/DC1.

REFERENCES

Ambati, B.K., M. Nozaki, N. Singh, A. Takeda, P.D. Jani, T. Suthar, R.J. Albuquerque, E. Richter, E. Sakurai, M.T. Newcomb, et al. 2006. Corneal avascularity is due to soluble VEGF receptor-1. *Nature*. 443:993–997. http://dx.doi.org/10.1038/nature05249

Bais, C., X. Wu, J. Yao, S. Yang, Y. Crawford, K. McCutcheon, C. Tan, G. Kolumam, J.M. Vernes, J. Eastham-Anderson, et al. 2010. PlGF block-ade does not inhibit angiogenesis during primary tumor growth. *Cell*. 141:166–177. http://dx.doi.org/10.1016/j.cell.2010.01.033

Beck, H., S. Raab, E. Copanaki, M. Heil, A. Scholz, M. Shibuya, T. Deller, M. Machein, and K.H. Plate. 2010. VEGFR-1 signaling regulates the homing of bone marrow–derived cells in a mouse stroke model. *J. Neuropathol. Exp. Neurol*. 69:168–175. http://dx.doi.org/10.1097/NEN.0b013e3181c9c05b

Borowsky, A.D., R. Namba, L.J. Young, K.W. Hunter, J.G. Hodgson, C.G. Tepper, E.T. McGoldrick, W.J. Muller, R.D. Cardiff, and J.P. Gregg. 2005. Syngeneic mouse mammary carcinoma cell lines: two closely re-lated cell lines with divergent metastatic behavior. *Clin. Exp. Metastasis*. 22:47–59. http://dx.doi.org/10.1007/s10585-005-2908-5

Byrne, P.V., L.J. Guilbert, and E.R. Stanley. 1981. Distribution of cells bearing receptors for a colony-stimulating factor (CSF-1) in murine tis-sues. *J. Cell Biol*. 91:848–853. http://dx.doi.org/10.1083/jcb.91.3.848

Casanovas, O., D.J. Hicklin, G. Bergers, and D. Hanahan. 2005. Drug re-sistance by evasion of antiangiogenic targeting of VEGF signaling in late-stage pancreatic islet tumors. *Cancer Cell*. 8:299–309. http://dx.doi.org/10.1016/j.ccr.2005.09.005

Chen, Q., X.H. Zhang, and J. Massagué. 2011. Macrophage binding to receptor VCAM-1 transmits survival signals in breast cancer cells that invade the lungs. *Cancer Cell*. 20:538–549. http://dx.doi.org/10.1016/j.ccr.2011.08.025

Chitu, V., and E.R. Stanley. 2006. Colony-stimulating factor-1 in immu-nity and inflammation. *Curr. Opin. Immunol*. 18:39–48. http://dx.doi.org/10.1016/j.coi.2005.11.006

Condeelis, J., and J.W. Pollard. 2006. Macrophages: obligate partners for tumor cell migration, invasion, and metastasis. *Cell*. 124:263–266. http://dx.doi.org/10.1016/j.cell.2006.01.007

Coussens, L.M., and J.W. Pollard. 2011. Leukocytes in mammary develop-ment and cancer. *Cold Spring Harb. Perspect. Biol*. 3:a003285. http://dx.doi.org/10.1101/cshperspect.a003285

Coussens, L.M., L. Zitvogel, and A.K. Palucka. 2013. Neutralizing tumor-promoting chronic inflammation: a magic bullet? *Science*. 339:286–291. http://dx.doi.org/10.1126/science.1232227

Curry, J.M., T.D. Eubank, R.D. Roberts, Y. Wang, N. Pore, A. Maity, and C.B. Marsh. 2008. M-CSF signals through the MAPK/ERK path-way via Sp1 to induce VEGF production and induces angiogenesis in vivo. *PLoS ONE*. 3:e3405. http://dx.doi.org/10.1371/journal.pone.0003405

Dawson, M.R., D.G. Duda, S.S. Chae, D. Fukumura, and R.K. Jain. 2009a. VEGFR1 activity modulates myeloid cell infiltration in growing lung metastases but is not required for spontaneous metastasis formation. *PLoS ONE*. 4:e6525. http://dx.doi.org/10.1371/journal.pone.0006525

Dawson, M.R., D.G. Duda, D. Fukumura, and R.K. Jain. 2009b. VEGFR1-activity-independent metastasis formation. *Nature*. 461:E4. http://dx.doi.org/10.1038/nature08254

De Palma, M., and C.E. Lewis. 2013. Macrophage regulation of tumor re-sponses to anticancer therapies. *Cancer Cell*. 23:277–286. http://dx.doi.org/10.1016/j.ccr.2013.02.013

Deng, L., J.F. Zhou, R.S. Sellers, J.F. Li, A.V. Nguyen, Y. Wang, A. Orlofsky, Q. Liu, D.A. Hume, J.W. Pollard, et al. 2010. A novel mouse model of inflammatory bowel disease links mammalian target of rapamycin-dependent hyperproliferation of colonic epithelium to inflammation-associated tumorigenesis. *Am. J. Pathol*. 176:952–967. http://dx.doi.org/10.2353/ajpath.2010.090622

Fidler, I.J. 2003. The pathogenesis of cancer metastasis: the 'seed and soil' hypothesis revisited. *Nat. Rev. Cancer*. 3:453–458. http://dx.doi.org/10.1038/nrc1098

Fischer, C., B. Jonckx, M. Mazzone, S. Zacchigna, S. Loges, L. Pattarini, E. Chorianopoulos, L. Liesenborghs, M. Koch, M. De Mol, et al. 2007. Anti-PlGF inhibits growth of VEGF(R)-inhibitor-resistant tumors without affecting healthy vessels. *Cell*. 131:463–475. http://dx.doi.org/10.1016/j.cell.2007.08.038

Gil-Bernabé, A.M., S. Ferjancic, M. Tlalka, L. Zhao, P.D. Allen, J.H. Im, K. Watson, S.A. Hill, A. Amirkhosravi, J.L. Francis, et al. 2012. Recruitment of monocytes/macrophages by tissue factor-mediated coagulation is essential for metastatic cell survival and premetastatic niche establishment in mice. *Blood*. 119:3164–3175. http://dx.doi.org/10.1182/blood-2011-08-376426

Grivennikov, S.I., F.R. Greten, and M. Karin. 2010. Immunity, inflamma-tion, and cancer. *Cell*. 140:883–899. http://dx.doi.org/10.1016/j.cell.2010.01.025

Hiratsuka, S., O. Minowa, J. Kuno, T. Noda, and M. Shibuya. 1998. Flt-1 lacking the tyrosine kinase domain is sufficient for normal development and angiogenesis in mice. *Proc. Natl. Acad. Sci. USA*. 95:9349–9354. http://dx.doi.org/10.1073/pnas.95.16.9349

Hiratsuka, S., K. Nakamura, S. Iwai, M. Murakami, T. Itoh, H. Kijima, J.M. Shipley, R.M. Senior, and M. Shibuya. 2002. MMP9 induction by vascular endothelial growth factor receptor-1 is involved in lung-specific metastasis. *Cancer Cell*. 2:289–300. http://dx.doi.org/10.1016/S1535-6108(02)00153-8

Hutchinson, J.N., and W.J. Muller. 2000. Transgenic mouse models of human breast cancer. *Oncogene*. 19:6130–6137. http://dx.doi.org/10.1038/sj.onc.1203970

Jemal, A., R. Siegel, J. Xu, and E. Ward. 2010. Cancer statistics, 2010. *CA Cancer J. Clin*. 60:277–300. http://dx.doi.org/10.3322/caac.20073

Joyce, J.A., and J.W. Pollard. 2009. Microenvironmental regulation of metastasis. *Nat. Rev. Cancer*. 9:239–252. http://dx.doi.org/10.1038/nrc2618

Kaplan, R.N., R.D. Riba, S. Zacharoulis, A.H. Bramley, L. Vincent, C. Costa, D.D. MacDonald, D.K. Jin, K. Shido, S.A. Kerns, et al. 2005. VEGFR1-positive haematopoietic bone marrow progenitors initiate the pre-metastatic niche. *Nature*. 438:820–827. http://dx.doi.org/10.1038/nature04186

Kitamura, T., B.Z. Qian, D. Soong, L. Cassetta, R. Noy, G. Sugano, Y. Kato, J. Li, and J.W. Pollard. 2015. CCL2-induced chemokine cascade promotes breast cancer metastasis by enhancing retention of metasta-sis-associated macrophages. *J. Exp. Med*. 212:1043–1059. http://dx.doi.org/10.1084/jem.20141836

Labelle, M., and R.O. Hynes. 2012. The initial hours of metastasis: the importance of cooperative host-tumor cell interactions during hema-togenous dissemination. *Cancer Discov*. 2:1091–1099. http://dx.doi.org/10.1158/2159-8290.CD-12-0329

Lin, E.Y., A.V. Nguyen, R.G. Russell, and J.W. Pollard. 2001. Colony-stimulating factor 1 promotes progression of mammary tumors to ma-lignancy. *J. Exp. Med*. 193:727–740. http://dx.doi.org/10.1084/jem.193.6.727

Lin, E.Y., J.G. Jones, P. Li, L. Zhu, K.D. Whitney, W.J. Muller, and J.W. Pollard. 2003. Progression to malignancy in the polyoma middle T onco-protein mouse breast cancer model provides a reliable model for human diseases. *Am. J. Pathol*. 163:2113–2126. http://dx.doi.org/10.1016/S0002-9440(10)63568-7

Lyden, D., K. Hattori, S. Dias, C. Costa, P. Blaikie, L. Butros, A. Chadburn, B. Heissig, W. Marks, L. Witte, et al. 2001. Impaired recruitment of bone-marrow-derived endothelial and hematopoietic precursor cells blocks tumor angiogenesis and growth. *Nat. Med*. 7:1194–1201. http://dx.doi.org/10.1038/nm1101-1194

Mantovani, A., and A. Sica. 2010. Macrophages, innate immunity and can-cer: balance, tolerance, and diversity. *Curr. Opin. Immunol*. 22:231–237. http://dx.doi.org/10.1016/j.coi.2010.01.009

Mantovani, A., P. Allavena, A. Sica, and F. Balkwill. 2008. Cancer-related inflammation. *Nature*. 454:436–444. http://dx.doi.org/10.1038/nature07205

McDermott, R.S., L. Deneux, V. Mosseri, J. Védrenne, K. Clough, A. Fourquet, J. Rodriguez, J.M. Cosset, X. Sastre, P. Beuzeboc, et al. 2002. Circulating macrophage colony stimulating factor as a marker of tumour progression. *Eur. Cytokine Netw.* 13:121–127.

Minn, A.J., G.P. Gupta, P.M. Siegel, P.D. Bos, W. Shu, D.D. Giri, A. Viale, A.B. Olshen, W.L. Gerald, and J. Massagué. 2005. Genes that mediate breast cancer metastasis to lung. *Nature*. 436:518–524. http://dx.doi.org/10.1038/nature03799

Murakami, M., Y. Zheng, M. Hirashima, T. Suda, Y. Morita, J. Ooehara, H. Ema, G.H. Fong, and M. Shibuya. 2008. VEGFR1 tyrosine kinase signaling promotes lymphangiogenesis as well as angiogenesis indirectly via macrophage recruitment. *Arterioscler. Thromb. Vasc. Biol.* 28:658–664. http://dx.doi.org/10.1161/ATVBAHA.107.150433

Murdoch, C., A. Giannoudis, and C.E. Lewis. 2004. Mechanisms regulating the recruitment of macrophages into hypoxic areas of tumors and other ischemic tissues. *Blood*. 104:2224–2234. http://dx.doi.org/10.1182/blood-2004-03-1109

Neve, R.M., K. Chin, J. Fridlyand, J. Yeh, F.L. Baehner, T. Fevr, L. Clark, N. Bayani, J.P. Coppe, F. Tong, et al. 2006. A collection of breast cancer cell lines for the study of functionally distinct cancer subtypes. *Cancer Cell*. 10:515–527. http://dx.doi.org/10.1016/j.ccr.2006.10.008

Nielsen, B.S., L.R. Lund, I.J. Christensen, M. Johnsen, P.A. Usher, L. Wulf-Andersen, T.L. Frandsen, K. Danø, and H.J. Gundersen. 2001. A precise and efficient stereological method for determining murine lung metastasis volumes. *Am. J. Pathol.* 158:1997–2003. http://dx.doi.org/10.1016/S0002-9440(10)64671-8

Olsson, A.K., A. Dimberg, J. Kreuger, and L. Claesson-Welsh. 2006. VEGF receptor signalling – in control of vascular function. *Nat. Rev. Mol. Cell Biol.* 7:359–371. http://dx.doi.org/10.1038/nrm1911

Peinado, H., M. Alečković, S. Lavotshkin, I. Matei, B. Costa-Silva, G. Moreno-Bueno, M. Hergueta-Redondo, C. Williams, G. García-Santos, C. Ghajar, et al. 2012. Melanoma exosomes educate bone marrow progenitor cells toward a pro-metastatic phenotype through MET. *Nat. Med.* 18:883–891. http://dx.doi.org/10.1038/nm.2753

Qian, B.Z., and J.W. Pollard. 2010. Macrophage diversity enhances tumor progression and metastasis. *Cell*. 141:39–51. http://dx.doi.org/10.1016/j.cell.2010.03.014

Qian, B., Y. Deng, J.H. Im, R.J. Muschel, Y. Zou, J. Li, R.A. Lang, and J.W. Pollard. 2009. A distinct macrophage population mediates metastatic breast cancer cell extravasation, establishment and growth. *PLoS ONE*. 4:e6562. http://dx.doi.org/10.1371/journal.pone.0006562

Qian, B.Z., J. Li, H. Zhang, T. Kitamura, J. Zhang, L.R. Campion, E.A. Kaiser, L.A. Snyder, and J.W. Pollard. 2011. CCL2 recruits inflammatory monocytes to facilitate breast-tumour metastasis. *Nature*. 475:222–225. http://dx.doi.org/10.1038/nature10138

Quail, D.F., and J.A. Joyce. 2013. Microenvironmental regulation of tumor progression and metastasis. *Nat. Med.* 19:1423–1437. http://dx.doi.org/10.1038/nm.3394

Richardsen, E., R.D. Uglehus, J. Due, C. Busch, and L.T. Busund. 2008. The prognostic impact of M-CSF, CSF-1 receptor, CD68 and CD3 in prostatic carcinoma. *Histopathology*. 53:30–38. http://dx.doi.org/10.1111/j.1365-2559.2008.03058.x

Roth, P., and E.R. Stanley. 1992. The biology of CSF-1 and its receptor. *Curr. Top. Microbiol. Immunol.* 181:141–167.

Ruffell, B., N.I. Affara, and L.M. Coussens. 2012. Differential macrophage programming in the tumor microenvironment. *Trends Immunol.* 33:119–126. http://dx.doi.org/10.1016/j.it.2011.12.001

Saeed, A.I., V. Sharov, J. White, J. Li, W. Liang, N. Bhagabati, J. Braisted, M. Klapa, T. Currier, M. Thiagarajan, et al. 2003. TM4: a free, open-source system for microarray data management and analysis. *Biotechniques*. 34:374–378.

Scholl, S.M., C. Pallud, F. Beuvon, K. Hacene, E.R. Stanley, L. Rohrschneider, R. Tang, P. Pouillart, and R. Lidereau. 1994. Anti-colony-stimulating factor-1 antibody staining in primary breast adenocarcinomas correlates with marked inflammatory cell infiltrates and prognosis. *J. Natl. Cancer Inst.* 86:120–126. http://dx.doi.org/10.1093/jnci/86.2.120

Scholl, S.M., R. Lidereau, A. de la Rochefordière, C.C. Le-Nir, V. Mosseri, C. Noguès, P. Pouillart, and F.R. Stanley. 1996. Circulating levels of the macrophage colony stimulating factor CSF-1 in primary and metastatic breast cancer patients. A pilot study. *Breast Cancer Res. Treat.* 39:275–283. http://dx.doi.org/10.1007/BF01806155

Shibuya, M. 2006. Vascular endothelial growth factor receptor-1 (VEGFR-1/Flt-1): a dual regulator for angiogenesis. *Angiogenesis*. 9:225–230. http://dx.doi.org/10.1007/s10456-006-9055-8

Sleeman, J., and P.S. Steeg. 2010. Cancer metastasis as a therapeutic target. *Eur. J. Cancer*. 46:1177–1180. http://dx.doi.org/10.1016/j.ejca.2010.02.039

Smith, H.O., P.S. Anderson, D.Y. Kuo, G.L. Goldberg, C.L. DeVictoria, C.A. Boocock, J.G. Jones, C.D. Runowicz, E.R. Stanley, and J.W. Pollard. 1995. The role of colony-stimulating factor 1 and its receptor in the etiopathogenesis of endometrial adenocarcinoma. *Clin. Cancer Res.* 1:313–325.

Stefater, J.A. III, I. Lewkowich, S. Rao, G. Mariggi, A.C. Carpenter, A.R. Burr, J. Fan, R. Ajima, J.D. Molkentin, B.O. Williams, et al. 2011. Regulation of angiogenesis by a non-canonical Wnt-Flt1 pathway in myeloid cells. *Nature*. 474:511–515. http://dx.doi.org/10.1038/nature10085

Tichelaar, J.W., W. Lu, and J.A. Whitsett. 2000. Conditional expression of fibroblast growth factor-7 in the developing and mature lung. *J. Biol. Chem.* 275:11858–11864. http://dx.doi.org/10.1074/jbc.275.16.11858

Toy, E.P., J.T. Chambers, B.M. Kacinski, M.B. Flick, and S.K. Chambers. 2001. The activated macrophage colony-stimulating factor (CSF-1) receptor as a predictor of poor outcome in advanced epithelial ovarian carcinoma. *Gynecol. Oncol.* 80:194–200. http://dx.doi.org/10.1006/gyno.2000.6070

Van Nguyen, A., and J.W. Pollard. 2002. Colony stimulating factor-1 is required to recruit macrophages into the mammary gland to facilitate mammary ductal outgrowth. *Dev. Biol.* 247:11–25. http://dx.doi.org/10.1006/dbio.2002.0669

Wiktor-Jedrzejczak, W., A. Bartocci, A.W. Ferrante Jr., A. Ahmed-Ansari, K.W. Sell, J.W. Pollard, and E.R. Stanley. 1990. Total absence of colony-stimulating factor 1 in the macrophage-deficient osteopetrotic (op/op) mouse. *Proc. Natl. Acad. Sci. USA*. 87:4828–4832. http://dx.doi.org/10.1073/pnas.87.12.4828

Wu, Y., Z. Zhong, J. Huber, R. Bassi, B. Finnerty, E. Corcoran, H. Li, E. Navarro, P. Balderes, X. Jimenez, et al. 2006. Anti-vascular endothelial growth factor receptor-1 antagonist antibody as a therapeutic agent for cancer. *Clin. Cancer Res.* 12:6573–6584. http://dx.doi.org/10.1158/1078-0432.CCR-06-0831

Wyckoff, J.B., Y. Wang, E.Y. Lin, J.F. Li, S. Goswami, E.R. Stanley, J.E. Segall, J.W. Pollard, and J. Condeelis. 2007. Direct visualization of macrophage-assisted tumor cell intravasation in mammary tumors. *Cancer Res.* 67:2649–2656. http://dx.doi.org/10.1158/0008-5472.CAN-06-1823

Supplemental Table 1

Antibody	Short Name in Fig 8	Supplier	Order Number
Akt	Akt	Cell Signaling Technologies	9272
Akt P Thr308	P-Akt	Cell Signaling Technologies	2965
c-Jun N-term	c-Jun	Epitomics	1254-1
c-Jun P Ser73	P-c-Jun	Cell Signaling Technologies	9164
ErbB-3/Her3/EGFR	ErbB-3	Cell Signaling Technologies	4754
ErbB-3/Her3/EGFR P Tyr1289	P-ErbB-3	Cell Signaling Technologies	4791
FAK1	FAK1	Cell Signaling Technologies	3285
FAK1 P Y397	P-FAK1	Cell Signaling Technologies	3283
FLT3 P Tyr591 P Tyr591	P-FLT3	Cell Signaling Technologies	3461
GSK-3-alpha/beta P Ser21/Ser9	P-GSK-3-alpha	Cell Signaling Technologies	9331
GSK-3-beta	GSK-3-beta	Cell Signaling Technologies	9315
GSK-3-beta P Ser9	P-GSK-3-beta	Cell Signaling Technologies	9336
MEK1/2	MEK1/2	Cell Signaling Technologies	9122
MEK1/2 P Ser217/221	P-MEK1/2	Cell Signaling Technologies	9154
mTOR	mTOR	Cell Signaling Technologies	2972
mTOR P Ser2448	P-mTOR[1]	Cell Signaling Technologies	2971
mTOR P Ser2481	P-mTOR[2]	Millipore (Upstate)	09-343SP
p38 MAPK	p38 MAPK	Cell Signaling Technologies	9212
p38 MAPK PThr180,Tyr182	P-p38 MAPK	Cell Signaling Technologies	9211
p44/42 MAPK (ERK1/2)	p44/42 MAPK	Cell Signaling Technologies	9102
p44/42 MAPK (ERK1/2) P Thr202/Thr185,Tyr204/Tyr187	P-p44/42 MAPK	Cell Signaling Technologies	4370
p70 S6 Kinase	p70 S6 Kinase	Cell Signaling Technologies	9202
p70 S6 Kinase P Thr389	P-p70 S6 Kinase[1]	Epitomics	1175-1
p70 S6 Kinase P Thr421,Ser424	P-p70 S6 Kinase[2]	Cell Signaling Technologies	9204
p90 S6 kinase (Rsk1-3)	p90 S6 kinase	Santa Cruz	sc-231
p90 S6 kinase (Rsk1-3) P Thr359,Ser363	P-p90 S6 kinase	Cell Signaling Technologies	9344
PI3 Kinase p110-alpha	PI3K	Cell Signaling Technologies	4249
PKC (pan) P Ser660 (beta-2)	P-PKC	Cell Signaling Technologies	9371
PKC substrate P (R/K)X(S*)(Hyd)(R/k)	PKC	Cell Signaling Technologies	2261
PKC-zeta	PKC-zeta	Cell Signaling Technologies	9372
PKC-zeta/lambda P Thr410/403	P-PKC-zeta/lambda	Cell Signaling Technologies	9378
PLC-gamma1	PLC-gamma1	Cell Signaling Technologies	2822
PLC-gamma1 P Tyr783	P-PLC-gamma1	Cell Signaling Technologies	2821
Prohibitin	Prohibitin	Santa Cruz	sc-28259
PTEN	PTEN	Cell Signaling Technologies	9552
PTEN P Ser380,Thr382,Thr383	P-PTEN	Cell Signaling Technologies	9554
Raf P Ser259	P-Raf[1]	Cell Signaling Technologies	9421
Raf P Ser338	P-Raf[2]	Cell Signaling Technologies	9427
Rsk2 Pser 227	P-Rsk2	Cell Signaling Technologies	3556
S6 Ribosomal Protein	S6 Ribosomal Protein	Cell Signaling Technologies	2217
S6 Ribosomal protein P Ser235,Ser236	P-S6 Ribosomal protein[1]	Cell Signaling Technologies	2211
S6 Ribosomal protein p Ser240,Ser244	P-S6 Ribosomal protein[2]	Cell Signaling Technologies	2215
SHP2 P Tyr542	P-SHP2	Cell Signaling Technologies	3751
Src	Src	Cell Signaling Technologies	2109
Src (family) P Tyr416	P-Src	Cell Signaling Technologies	2101